Genesis of End-to-End Chromosome Fusions

Mia Rochelle Lowden

A dissertation submitted to the faculty of the University of North Carolina at Chapel Hill in partial fulfillment of requirements for the degree of Doctor of Philosophy in the Department of Biology.

Chapel Hill
2008

Approved by:
Shawn Ahmed
Jack Griffith
Mike Jarstfer
Jeff Sekelsky
Bob Goldstein

ABSTRACT

Mia Rochelle Lowden: Genesis of End-to-End Chromosome Fusions
(Under the direction of Dr. Shawn Ahmed)

Telomeres are DNA-protein complexes that form a protective cap at chromosome ends and provide a buffer against gradual loss DNA that occurs with every round of DNA replication. Telomere length is replenished by telomerase. Deficiency of telomerase in most human somatic cells causes telomere shortening with age. When telomeres become critically short, they uncap and can be processed as abnormal double strand breaks to generate end-to-end chromosome fusions. The resulting dicentric chromosomes may promote tumorigenesis, but they enter fusion-breakage-bridge cycles that impede the elucidation of the structure of the initial fusion event and a mechanistic understanding of their genesis.

Current models for fusion of critically shortened, uncapped telomeres rely on PCR-based assays that typically capture fusion breakpoints created by ligation of two chromosome ends. We used two independent approaches that rely on distinctive features of the nematode *C. elegans* to study the frequency of direct end-to-end chromosome fusions in telomerase mutants: 1) holocentric chromosomes that allow for genetic isolation of stable end-to-end fusion events, and 2) unique subtelomeric sequences that allow for an unbiased, nearly exhaustive PCR analysis of samples of genomic DNA harboring multiple end-to-end fusions. Surprisingly, only a minority of initial end-to-end fusion events resulted from direct end-joining with no other rearrangements. We used three

approaches to investigate complex fusion breakpoint structures: 1) physical analysis of the fusion breakpoint DNA by Southern blotting, 2) measurement of DNA copy number by microarray analysis, and 3) sequence analysis of fusion breakpoints recovered by inverse PCR. Duplications as large as two megabases were present at complex fusion breakpoints. Such events would have been missed by studies using typical PCR-based assays. Thus, duplications of various segments of the genome may be a major factor that drives end-to-end chromosome fusion and promotes tumor development.

For my parents Rhonda and Michael Lowden:

Thank you.

ACKNOWLEDGEMENTS

To my parents: Your love and support of me and each other made me who I am and made this accomplishment possible.

To my family, thank you for your love and support. Even though I was far away, you were always in my heart, and you let me know I was in yours.

To Shawn: From your response to my first email enquiring about a rotation and throughout my time in lab, you have shown enthusiasm for science. You made my transition from chemistry to genetics easy by teaching me techniques and analysis which gave me a solid foundation to be more independent as I went along. I appreciate your encouragement and assistance with my fellowship applications. That experience helped me learn about designing a research project and improve my writing.

I thank my thesis committee for be helpful and supportive. My meetings with you felt like a group getting together to brainstorm on how to best push my project forward and I left each one feeling more motivated and excited about science.

Sharon, I always called you Super Woman because of your amazing juggling act of roles and responsibilities. Somehow, you found the time to be a mentor to me as well. I benefited from your guidance even before I started graduate school because you encouraged me to the IBMS program. Thank you for your advice over the years.

Thank you to the past and present members of the Ahmed lab for your help with techniques, discussions about science, and encouragement.

I made many friends at Carolina to share the experience of graduate school. Stephanie and I did everything together, from working out to shopping. I was lucky to have you a step ahead of me because you were happy to share your knowledge and make my path easier. Yvette was always just down the hall when I wanted to talk about science or life, and up for fun on the weekends. Your smiles and stories brightened my days. Nihal, showed me generosity that helped me better understand all that a friend can be. Thank you for sharing your culture with me and for all the chats about science and family life. We each lived far from our families and it was helpful to talk to you about that experience. I seemed to run into Matt randomly, just when I needed his perspective and reassurance. I looked forward to the parties that you and Ally threw as a chance to unwind and meet the your great circle of friends. Karen and Drew, I enjoyed our conversations. Hanging out with you was rejuvenating. Nate and Melvyn, I am very glad I found you. You made my time at Carolina happier and easier.

Before Carolina, there was Carleton. Domineke, having you to talk with through this experience was a source of strength. We took very different paths, yet experienced similar feelings after Carleton. Thank you for your wisdom, your patience, and for being on my biggest cheer leaders. Rietta and Hudlin, I feel blessed to have you in my life. Your guidance did not end when I left Carleton, but followed me and boosted me throughout graduate school. Trish, thank you for being a mentor and an example offering your perspective as a woman in science.

Joshua, having you by my side was a great help. You saw me through every up and down with firm encouragement, a positive outlook, and love. Thank you.

TABLE OF CONTENTS

LIST OF TABLES

LIST OF FIGURES

LIST OF ABBREVIATIONS AND SYMBOLS

%	percent
°C	degree Celsius
#	number
bp	basepair
C. elegans	*Caenorhabditis elegans*
DAPI	4’,6-diamidino-2-phenylindole
DSB	double-strand break
DNA	deoxyribonucleic acid
IR	ionizing radiation
IL	left end of chromosome *I*
IR	right end of chromosome *I*
IIL	left end of chromosome *II*
IIR	right end of chromosome *II*
IIIL	left end of chromosome *III*
IIIR	right end of chromosome *III*
IVL	left end of chromosome *IV*
IVR	right end of chromosome *IV*
kb	kilobase
Mrt	mortal germline
MRN	Mre11/Rad50/NBS1 complex
NGM	nematode growth medium

NHEJ	non-homologous end-joining
P	*P*-value
PCNA	proliferating cell nuclear antigen
PCR	polymerase chain reaction
RNA	ribonucleic acid
RNAi	RNA interference
t-loop	telomeric loop
VL	left end of chromosome *V*
VR	right end of chromosome *V*
XL	left end of *X* chromosome
XR	right end of *X* chromosome

CHAPTER 1

INTRODUCTION

Telomere function

Upon X-ray irradiation of eukaryotic chromosomes, broken chromosome ends fuse to each other, but natural chromosome ends avoid these fusion events (McClintock, 1941; Müller, 1938). This remarkable feature of natural chromosome ends was first described by Hermann Müller and Barbara McClintock, who converged upon the same discovery while studying chromosome dynamics in the fruit fly *Drosophila melanogaster* and in maize, respectively. Müller named the natural ends of chromosomes telomeres (Müller, 1938). Though both researchers extensively studied rearrangement of broken chromosomes with genetics and cytology, neither had the tools to explain the protective function of telomeres at the molecular level. Discovery of the structure of DNA and mechanisms of DNA replication exposed an additional threat for telomeres to guard against: progressive telomere shortening. DNA replication occurs in two coupled modes termed leading and lagging strand replication such that the daughter of leading strand replication is synthesized processively, while the daughter of lagging strand replication is synthesized in short stretches that are later ligated to form a continuous DNA strand. For the lagging strand, DNA polymerase α initiate de novo DNA synthesis by extending RNA primers generated by primase. Primase typically does not place primers at the end

of the telomere, thus the region between the most distal primer and the end of the telomere is not replicated. In addition, after the most distal RNA primer is degraded, the gap at the telomere is further increased. Thus telomeres shorten progressively with every round of DNA replication, and a 3' overhang persists at the telomere. (Figure 1.1) (Kornberg, 1974; Ohki et al., 2001; Watson, 1972; Watson and Crick, 1953; Wright et al., 1997). This is known as the end replication problem (Olovnikov, 1973; Watson, 1972). Still, without more insight into telomere structure, the mechanism of telomere function was unclear.

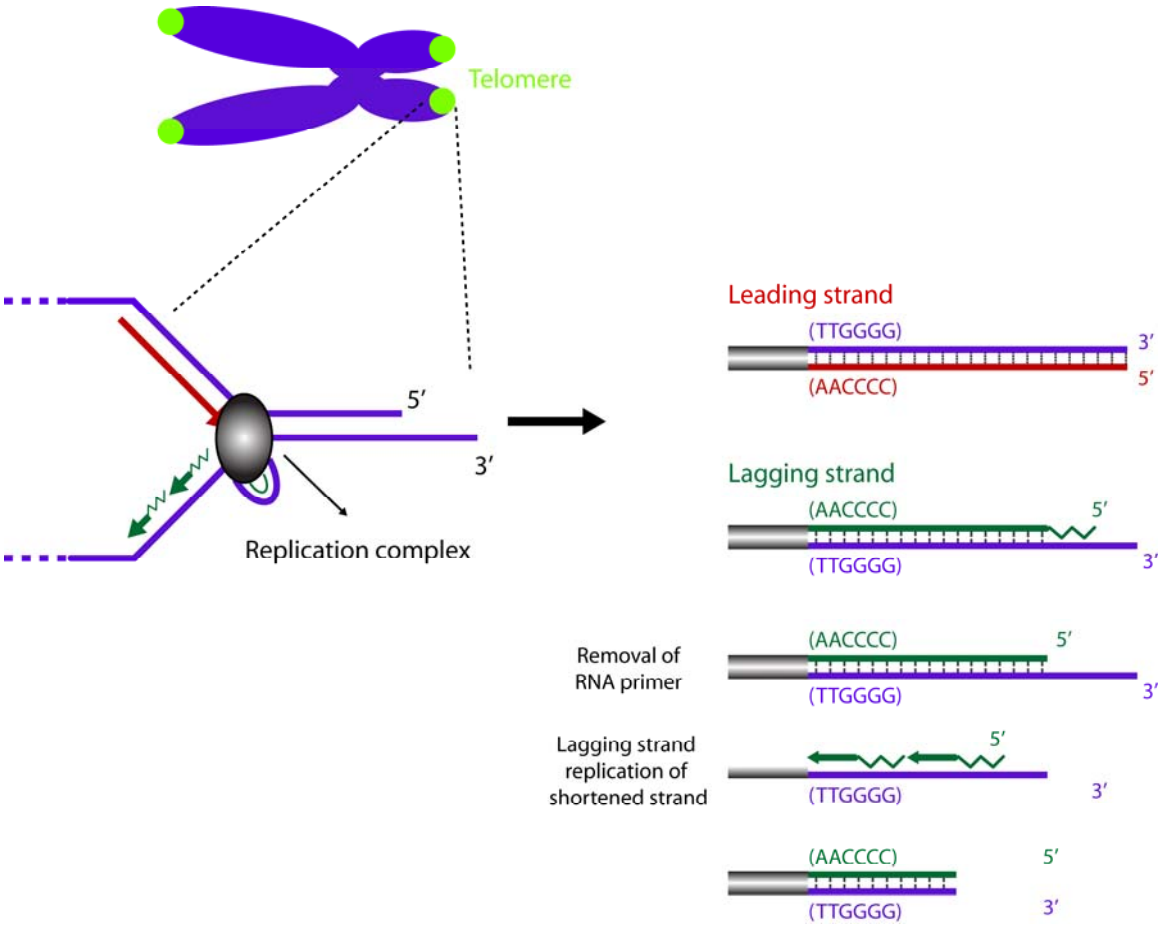

Figure 1.1: End replication problem

Do to the placement and degradation of the RNA used to prime DNA synthesis, telomeres shorten with each round of lagging strand replication. Telomeres buffer against the loss of vital sequences.

Telomere structure

DNA Sequence

Once methods for sequencing DNA were invented, it was possible to seek a deeper molecular understanding of telomeres (Sanger et al., 1977). Telomeric DNA was first sequenced using the ciliated protozoan *Tetrahymena thermophila*, which carries minichromosomes consisting of two copies of an rDNA gene flanked by telomeric DNA, such that many short, nearly identical molecules provide an abundance of telomeric DNA to study (Blackburn and Gall, 1978). In *Tetrahymena*, telomeric DNA is composed of 20 to 70 tandem repeats of the sequence TTGGGG running 5' to 3' toward the chromosome end (Blackburn and Gall, 1978). Cloning and sequencing telomeres has shown that telomere sequence is conserved among most eukaryotes and features short (usually 5-8 bp), tandem repeats of guanine rich DNA (reviewed in Brown et al., 1990). For example, telomere sequences in humans and *C. elegans* vary by one nucleotide: TTAGGG and TTAGGC, respectively (Moyzis et al., 1988; Wicky et al., 1996). Among vertebrates, telomere sequence is highly conserved: a human telomere probe detects telomeres in metaphase spreads from 91 vertebrate species (Moyzis et al., 1988). However, one organism with a strikingly different telomere sequence is *Drosophila*, which has non-long terminal repeat retrotransposons as telomeres (Levis et al., 1993). The repetitive nature of telomeric sequence suggests that it is non-coding DNA, which makes telomeres well-suited for their role as buffers against gradual sequence loss.

Protein components

In addition to telomeric DNA, a variety of proteins are required for chromosome end protection via telomeres. Some of these proteins specifically interact with telomeric

DNA, while others were originally characterized as DNA repair proteins and were later found to impact telomere biology. In the former category are the six components of the shelterin complex that shapes and protects human telomeres: two double-stranded DNA Telomere Repeat-binding Factors (TRF1 and TRF2), a telomeric 3' overhang binding factor Protection Of Telomeres 1 (POT1) and three proteins that interconnect the telomeric DNA-binding proteins (TIN2, Rap1, and TPP1) (reviewed in de Lange, 2005). POT1 may be conserved in nearly all eukaryotes (Baumann and Cech, 2001; Shakirov et al., 2005). The TRF1/2 and Rap1 are conserved in many species, while TIN2 and TPP1 are specific to vertebrates (reviewed in de Lange, 2005). Given that telomeres avoid DNA repair events that occur at double-strand breaks, such as homologous recombination (HR) and Non-Homologous End-Joining (NHEJ), interactions between telomeres and DNA repair proteins are surprising. Nevertheless, at least 14 DNA repair proteins affect telomere stability, including the Mre11-Rad50-NBS1 complex and the DNA-dependent Protein Kinase complex (Ku70, Ku80, and DNA-PK catalytic subunit), which are involved in HR and NHEJ, respectively (reviewed in Slijepcevic, 2006). Thus, a functional telomere is composed of DNA and proteins that coat or interact with the telomeric DNA.

G-rich 3' overhang

The daughter strands of both leading and lagging DNA replication have 3' overhangs, although the end replication problem predicts that only the daughter of lagging strand replication will have a 3' overhang, left behind after removal of the RNA primer used for DNA replication. A possible explanation for this is active processing of the leading strand can generate 3' overhangs. The leading strand has overhangs half or a

third as long as the lagging strand (Zhao et al., 2008). In addition, 80% of overhangs at the leading strand end with the same nucleotide, whereas overhangs at the lagging strand end more variably (Sfeir et al., 2005). Taken together, these results suggest that processing events generate the overhangs at leading strands, although the mechanisms of processing overhangs remasin unclear (Sfeir et al., 2005).

Telomere-loop

POT1 protects the 3' telomeric overhang and TRF2 remodels telomeric double-stranded DNA and the 3' overhang into a telomere loop (t-loop), a strand invasion configuration whereby the extreme tip of the chromosome is protected from exonucleolytic degradation and aberrant DNA repair (Griffith et al., 1999; Stansel et al., 2001; Yang et al., 2005). T-loops are highly conserved, although the size of the loop varies widely between species (e.g. 1 kb loops in trypanosomes and 50 kb loops in peas) (reviewed in de Lange, 2004). Thus, even the architecture of the telomere may play a role in its protective function.

Telomere lengthening

Most eukaryotic telomeres shorten at a rate of 4 to 200 nucleotides per cell division due to the end replication problem, exonucleolytic processing, and oxidative damage (reviewed in Lydall, 2003; von Zglinicki et al., 2000). Telomere length is maintained by telomerase, a ribonucleoprotein complex that uses an RNA template and a reverse transcriptase to add telomeric repeats to chromosome ends (Figure 1.2) (Lingner et al., 1997; Shippen-Lentz and Blackburn, 1990; reviewed in Smogorzewska and de Lange, 2004). Most of telomeric DNA is replicated by standard DNA replication machinery. Telomerase extends the G-rich leading strand of telomeric DNA and then the

C-rich strand is filled in by standard lagging strand replication (Diede and Gottschling, 1999; Greider and Blackburn, 1987). In agreement with the conservation of the sequence of its telomeric DNA substrate, the telomerase reverse transcriptase and RNA subunits have been identified in highly divergent organisms (reviewed in Cech, 2004).

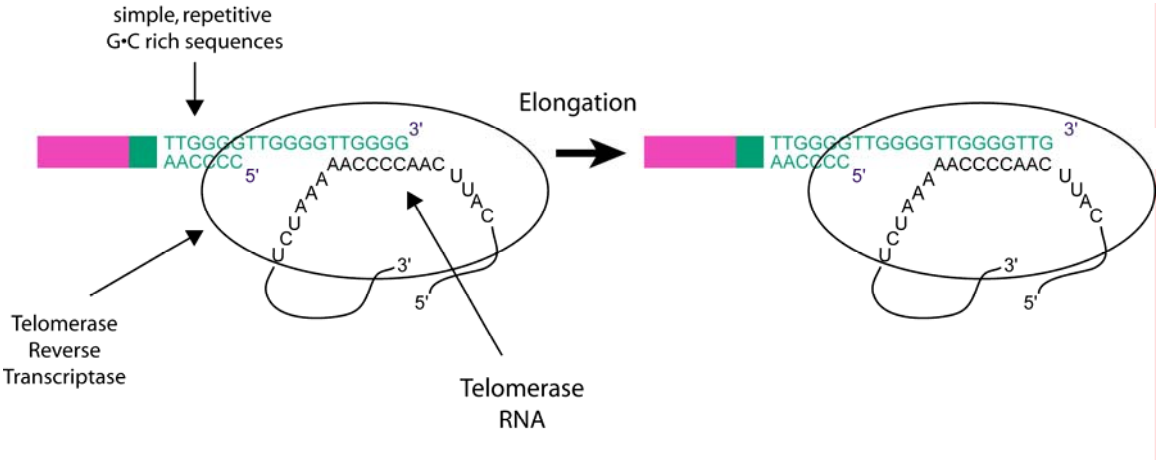

Figure 1.2: The enzyme telomerase adds telomeric DNA chromosome ends.

In the absence of telomerase, yeast and mammalian cells can maintain telomere length via Alternative Lengthening of Telomeres (ALT). In ALT-positive tumor cells, telomeric DNA sequences are copied from one telomere to another, thus ALT occurs by recombination (Dunham et al., 2000). ALT-associated ProMyelocytic Leukemia (PML) bodies localize in the nucleus and contain many factors that may facilitate recombination at telomeres including homologous recombination DNA repair proteins (the MRN complex, RAD51, RAD52), DNA replication factor A, helicases WRN and BLM, TRF1, TRF2, and telomeric DNA (reviewed in Henson et al., 2002; Lombard and Guarente, 2000; Wu et al., 2000; Yeager et al., 1999). In human cells, ALT is telomere specific, as

it does not affect the rate of recombination at internal chromosomal sites (Bechter et al., 2003).

Telomere length regulation

Telomeres maintained by ALT can vary widely in length as recombination generates sudden lengthening and deletion events (Murnane et al., 1994). In contrast, telomeres maintained by telomerase stay in a narrow range that varies by species and cell type, ranging from <30 bp in ciliates to ~50 kb in mice (reviewed in Hug and Lingner, 2006; Kipling and Cooke, 1990). The mechanisms underlying regulation of telomere length is an area of active study. There is evidence for genetic regulation of telomere length in yeast, maize, and mice (reviewed in Burr et al., 1992; Walmsley and Petes, 1985; Zhu et al., 1998). POT1, TRF1, TRF2 and proteins that interact with TRF1 are proposed to negatively regulate telomere length via a feedback mechanism whereby long telomeres containing sufficient amounts of TRF1 or POT1 proteins can inhibit recruitment of telomerase (without affecting levels of telomerase expression) while short telomeres presenting less TRF1 or POT1 can be extended by telomerase (Loayza and De Lange, 2003; Smogorzewska et al., 2000). Consistent with this possibility, longer telomeres contain greater amounts of POT1 and TRF1, and telomerase preferentially elongates the shortest telomeres in cells (Teixeira et al., 2004; van Steensel and de Lange, 1997).

Consequences of telomerase deficiency

Senescence and crisis

In most human somatic cells, telomerase expression is too low to maintain telomere length (Allsopp et al., 2001; Broccoli et al., 1995; Harle-Bachor and Boukamp,

1996; Hiyama et al., 1995; Liu et al., 1999; Masutomi et al., 2003; Son et al., 2000; Yasumoto et al., 1996). In this telomerase-deficient setting, telomere shortening with each cell division is proposed to account for the limited replicative capacity of human cells, possibly due to crossing a threshold telomere length that triggers a growth arrest phenotype termed senescence (Harley et al., 1990; Hayflick and Moorhead, 1961). Consistent with this prospect, critically shortened telomeres activate a persistent DNA damage response during senescence, analogous to well-characterized transient responses elicited by ionizing-radiation-induced Double-Strand Breaks (DSBs) (d'Adda di Fagagna et al., 2003; Gire et al., 2004; reviewed in Reaper et al., 2004). Persistent DNA damage signaling enforces a senescent phenotype where cells remain viable, metabolically active, and resistant to apoptosis (reviewed in Foreman and Tang, 2003; Wang, 1995).

Senescence can be bypassed by abrogation of cell-cycle checkpoint pathways due to loss of checkpoint proteins such as p53 or p16/Rb (Jarrard et al., 1999; Kiyono et al., 1998). In this setting, cells can continue dividing until critically shortened telomeres trigger crisis, a devastating state which is characterized by end-to-end chromosome fusions, breakage-fusion-bridge cycles and apoptosis (McClintock, 1941; reviewed in Shay et al., 1991). About 1 in 10^7 cells escape crisis by regaining the ability to lengthen telomeres (reviewed in Shay and Wright, 2005). Thus, after going through a process that introduces genomic alterations, cells can achieve immortality (Wright and Shay, 1992).

Molecular analysis of end-to-end chromosome fusions

The genesis of end-to-end chromosome fusions is of interest because the initial fusion events or the genomic instability associated with the ensuing breakage-fusion-bridge cycles may help to set the stage for tumorigenesis (McClintock, 1941; Murnane

and Sabatier, 2004). These genome rearrangements may result in *deletions*, which precipitate loss of heterozygosity, *translocations*, which place genes in a new context away from repressors or close to enhancers, and *duplications,* which may provide the raw material for gene amplification. Molecular analysis of end-to-end chromosome fusion breakpoints could reveal which DNA repair pathways mediate fusion events. Since uncapped telomeres elicit a DNA damage response like ionizing radiation-induced DSBs, they may be substrates for the major DSB repair pathways HR or NHEJ (Shrivastav et al., 2008). The unstable nature of dicentric chromosomes impedes analysis of fusion breakpoints. Nevertheless, PCR-based analysis of fusion breakpoints, followed by sequencing, has revealed molecular structures of fusion breakpoints in yeast, plants, worms, mice, and humans. All of these studies rely on PCR using primers adjacent to chromosome ends to amplify fusions from genomic template DNA that contains unknown quantities of end-to-end fusions (Capper et al., 2007; Cheung et al., 2006; Hackett et al., 2001; Heacock et al., 2004; Hemann et al., 2001; Mieczkowski et al., 2003). The results of these six studies are described in detail below.

PCR-analysis of fusion breakpoints in *Saccharomyces cerevisiae est1Δ* mutants, which are deficient for a protein required for telomerase activity in vivo, can recover fusion breakpoint sequences that are consistent with direct ligation of chromosome ends (Hackett et al., 2001). For all fusion events, terminal deletions ranging from 29 to 7379 bp occurred at both chromosome ends. 7 of 12 fusion breakpoints contained 1 to 10 bp of microhomology. Similar fusion events are recovered from $mTR^{-/-}$ mice which are deficient for the RNA subunit of telomerase: subtelomere-subtelomere fusions with terminal deletions at both chromosome ends and microhomology occurred for every

fusion breakpoint (n=8) (Hemann et al., 2001). The microhomology found at some fusion breakpoints might point to the mechanism of fusion, however this was not tested using the biochemical or genetic approaches used to establish Microhomology-Mediated End-Joining (MMEJ) as an alternative to NHEJ in *S. cerevisiae, Schizosaccharomyces pombe*, *Arabidobsis thaliana*, and mammalian cells and show that MMEJ typically relies on a minimum of 5 nucleotides homology (Bentley et al., 2004; Boulton and Jackson, 1996b; Decottignies, 2007; Feldmann et al., 2000; Guirouilh-Barbat et al., 2004; Heacock et al., 2004; Kabotyanski et al., 1998; Ma et al., 2003; Manolis et al., 2001; Tsuji et al., 2004; Yu and Gabriel, 2003; Zhong et al., 2002).

S. cerevisiae mec1 tel1 strains, which are deficient for homologues of ATR and ATM (two proteins involved in recognition and signaling to repair DSBs), accumulate end-to-end fusion events involving telomere sequences (Mieczkowski et al., 2003). Three types of fusion events were recovered: telomere-telomere (57%) and telomere-subtelomere (43%), and no fusion breakpoints exhibited microhomology. However, since telomere-telomere fusion creates inverted repeats that are refractory to sequencing, it is only possible to completely sequence telomere-telomere fusions with less than 100 bp of telomeric DNA at the fusion breakpoint. Also, since the primers used in this study were at most 150 bp from the telomere tracts, this set the upper limit of deletion that could be detected. The fusion breakpoint sequences are consistent with direct ligation events.

In *Arabidopsis*, *C. elegans*, and cultured human cells, both direct and complex (i.e. containing an insertion of genomic DNA) end-to-end chromosome fusions are recovered (Capper et al., 2007; Cheung et al., 2006; Heacock et al., 2004). In *Arabidopsis* telomerase mutants, direct fusion events occurred in three configurations: telomere-

telomere (11%), telomere-subtelomere (78%), and subtelomere-subtelomere (11%) (n=37) (Heacock et al., 2004). The fusion breakpoint sequences revealed terminal deletions (0 to 360 bp of subtelomeric DNA) and insertions (1 to 145 bp) occur, two hallmarks of NHEJ. Also, 38% of fusion breakpoints exhibited microhomology. One complex breakpoint was recovered, and it was a telomere-subtelomere fusion event containing a duplication of 69 bp of subtelomeric sequence plus some telomeric repeats from a chromosome end. In *C. elegans* telomerase mutants, direct fusion events have either a subtelomere-subtelomere configuration with microhomology at the breakpoint or a telomere-subtelomere configuration without microhomology (n=3) (Cheung et al., 2006). Complex fusion events involved duplications of 50 bp to 3800 bp (n=5). Finally, in human fibroblasts infected with human papilloma virus, which allows the cells to bypass senescence by abrogating the function of p53 and p16, both direct and complex fusion events exhibit terminal deletions up to 3010 bp which entirely removed the canonical telomeric repeat tracts at both chromosome ends at every fusion breakpoint (n=60 unique fusion events) (Capper et al., 2007). Although 72% of human fusion breakpoints contain telomere variant repeats which normally occur adjacent to canonical telomeric repeat tracts, variant repeats probably do not confer telomere function as they are not recognized by telomere binding proteins TRF1, TRF2, or POT1 (Capper et al., 2007). 1 to 49 bp of microhomology occurs at 89% of fusion breakpoints. 15% of fusion breakpoints are complex and contain duplications of 49 to 1650 bp. The complex fusion breakpoints recovered in these studies suggest that direct ligation is not the only outcome for uncapped telomeres. However, PCR-based analysis of unstable fusion breakpoints can reveal only what is happening at one breakpoint of a given fusion event, and does not

address whether that one breakpoint provides a full picture of the rearrangements involved in an end-to-end fusion. Furthermore, complex fusion breakpoints that are refractory to PCR might be missed. Thus, these studies cannot show the frequency of direct versus complex fusion events. To bypass some of the limitations encountered in the above studies, we analyzed genetically isolated end-to-end fusion events from *C. elegans* telomere replication mutants.

Goals of Dissertation

In *C. elegans* telomere replication mutants, including several alleles of the *trt-1* telomerase reverse transcriptase, telomere attrition over successive generations causes end-to-end chromosome fusions (Figure 1.3) (Ahmed and Hodgkin, 2000; Meier et al., 2006). End-to-end fusions that arise in *C. elegans* avoid the instability inherent to dicentric chromosomes because the chromosomes of *C. elegans* are holocentric, meaning that the mitotic spindle attaches along the entire chromosome (Albertson and Thomson, 1993). Furthermore, most end-to-end fusion events that arise in *C. elegans* telomere replication mutants are homozygous viable, allowing for genetic isolation of fusion events.

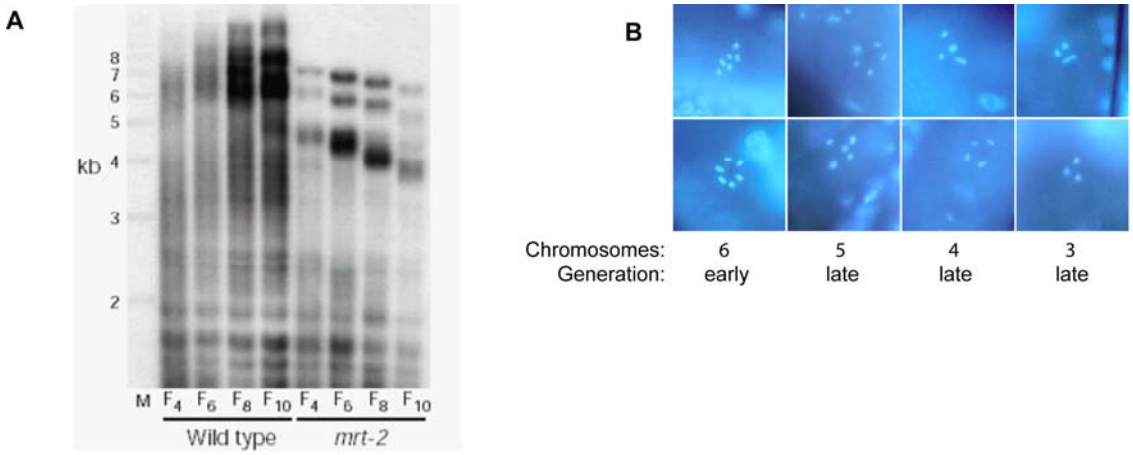

Figure 1.3: Phenotypes of telomerase mutants

A) Telomeres shorten over successive generations in *C. elegans* telomerase mutants. As shown by Southern analysis with a *C. elegans* telomere probe. B) DAPI-staining reveals that oocyte nuclei from late-generation telomerase mutants have few pairs of chromosomes than the wild-type complement of six chromosome pairs, indicating that chromosome fusions occurred.

Presented here are molecular structures of end-to-end fusion breakpoints from genetically isolated fusion events in *C. elegans*. The primary goal was to sequence fusion breakpoints and look for signatures of DNA repair pathways that create end-to-end fusion events.

An additional project described here investigated the role of Ku at telomeres in *C. elegans*. Ku is a multifunctional protein heterodimer with well-conserved roles in NHEJ and less clear roles in telomere biology. Chapter 2 describes in detail what is known

about Ku at telomeres in various species and our findings that Ku plays no apparent role at telomeres in *C. elegans*.

CHAPTER 2

NO ROLE FOR KU HETERODIMER AT TELOMERES IN *C. ELEGANS*

Preface

This chapter describes investigation of the effect of disrupting cku-80 and cku70, which encode components of the Ku heterodimer, a core component of NHEJ. I carried out the Southern blot analysis to determine telomere length and rate of telomere shortening. For one Southern blot measuring telomere length, the probe was prepared by Julie Hal. The results are included in an article that is currently under review at Genetics.

Background and Significance

Although natural chromosome termini avoid double-strand break (DSBs) repair events, several proteins that detect and repair DSBs localize at normal telomeres and some are required for telomere maintenance (reviewed in Slijepcevic, 2006). Two categories of DNA repair can act at DSB: homologous recombination (HR, which relies on sequence homology to guide repair) and non-homologous end-joining (which can join broken ends that lack extensive homology). Core components of both HR and NHEJ have been implicated in telomere function and among these the Ku heterodimer is one of the most studied and controversial (reviewed in Fisher and Zakian, 2005; reviewed in Slijepcevic, 2006). Ku is essential for canonical NHEJ. In vertebrates, the Ku heterodimer (Ku70 and Ku80) associates with DNA-dependent Protein Kinase catalytic subunit (DNA-PKcs), Artemis, DNA Ligase IV and XRCC4, which work together with other proteins to

process, align and ligate broken chromosomes (reviewed in Lieber, 1999). Genetic analyses of the role of Ku at normal telomeres in yeast, plants and vertebrates revealed that Ku deficiency has phenotypes ranging from no effect to altered telomere length and end-to-end fusion. Similarly, the impact of Ku deficiency in a telomerase-deficient background causes phenotypes ranging from no synthetic effect to synthetic lethality or accelerated telomere shortening.

Here, we assess whether NHEJ proteins play roles in telomere maintenance in *Caenorhabditis elegans*. Mutation of the *C. elegans* genes encoding telomerase reverse transcriptase TRT-1 or members of the 9-1-1 DNA damage response complex or its large replication factor C clamp loader subunit HPR-17 results in telomere shortening over successive generations, end-to-end chromosome fusions, and progressive sterility due telomerase deficiency (Ahmed and Hodgkin, 2000; Boerckel et al., 2007; Hofmann et al., 2002; Meier et al., 2006). *C. elegans* NHEJ mutants showed no telomere defects, nor did NHEJ affect telomere erosion or fusion in *trt-1* telomerase mutants.

Materials and Methods

Strains

All experiments were carried out at 20°C under standard culture conditions. The following strains were used in this study: N2 wild type, *trt-1(ok410) I*, *lig-4(tm750) III*, *lig-4(ok416) III*, *cku-80(tm1203) III*, *cku-80(ok861) III*, *cku-70(tm1524) III*, and *pot-1*(*tm1620*) *III*. Double mutants for *trt-1* with *cku-80*, *cku-70*, and *lig-4* were constructed by crossing *NHEJ* mutant males with *trt-1,unc-29* hermaphrodites and selecting for Unc F2 whose F3 embryos all displayed an Egg Radiation Sensitive phenotype characteristic

of *NHEJ* mutants (i.e. slow growth, vulval defects, and movement defects upon irradiation) (Clejan et al., 2006).

Telomere length analysis

Genomic DNA was prepared using a Puregene DNA Isolation Kit (Gentra). DNA was digested with *Hin*FI and separated on a 0.6% agarose gel at 1.5 *V*/cm. Southern blotting was carried out with a digoxigenin-dUTP-labeled probe following the manufacturer's instructions (Roche). Probe was made by PCR using primers Tel2 and T7long to amplify telomeric repeats from the plasmid cTel55X, as described (Wicky et al., 1996).

Results

Telomere length in NHEJ mutants

In *S. cerevisiae*, *S. pombe*, *K. lactis*, and *Arabidopsis*, the Ku heterodimer is required to maintain telomeres of normal length (Baumann and Cech, 2000; Boulton and Jackson, 1996a; Boulton and Jackson, 1996b; Carter et al., 2007; Riha et al., 2002). Conflicting data exist in mammals regarding the involvement of Ku in telomere length regulation, whereas spontaneous fusions are observed consistently in *ku70*- or *ku80*-mutant mice (though not in yeast, plants or chickens) (Bailey et al., 1999; d'Adda di Fagagna et al., 2001; Difilippantonio et al., 2000; Gilley et al., 2001; Goytisolo et al., 2001; Maser et al., 2007; Samper et al., 2000). To address the role of the Ku heterodimer at telomeres in *C. elegans*, strains harboring deletions in *cku-70 (tm1524)*, *cku-80 (tm1203* or *ok861)*, or *lig-4 (ok416* or *tm750)*, each of which confers a strong NHEJ DSB repair defect (Clejan et al., 2006), were outcrossed multiple times versus wild type.

Homozygous mutant lines were established and then examined for chromosome fusions or changes in telomere length. Propagation of these strains for 30 generations did not result in sterility, as occurs for telomerase mutants, nor in even modest drops in brood size . Furthermore, the NHEJ mutants failed to exhibit even low levels of dominant High Incidence of Males (Him) or embryonic lethal phenotypes indicative of chromosome missegregation, which occurs during meiosis when chromosome fusions are heterozygous (Herman et al., 1982). To assess telomere length, genomic DNA was isolated from *cku-70*, *cku-80*, or *lig-4* mutant strains and subjected to Southern analysis with a *C. elegans* $(TTAGGC)_n$ telomere repeat probe. For each allele, multiple independently outcrossed homozygous mutant lines were examined. Telomere length for *cku-70*, *cku-80* and *lig-4* mutants was similar to that of wild type, with telomeres ranging from 2 to 7 kb (Figure 2.1A and data not shown). In contrast, *pot-1(tm1620)* is an example of a mutation that elicits a significant increase in telomere length by generation F8 (Figure 2.1A). Thus, mutation of *C. elegans* genes encoding NHEJ proteins does not affect telomere length or result in spontaneous end-to-end fusions.

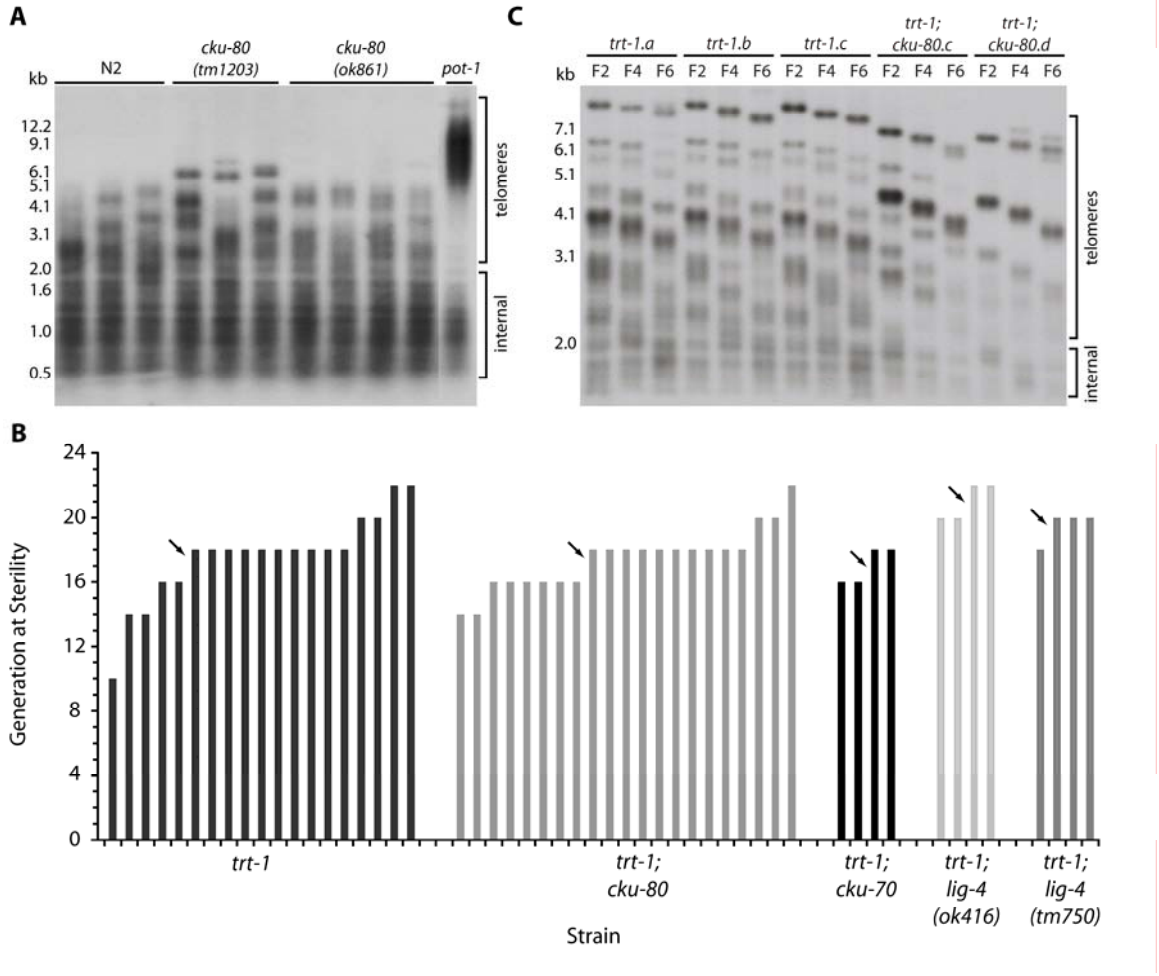

Figure 2.1: Ku-deficiency has no affect on *C. elegans* telomeres

A) Telomere length of *cku-80* mutant strains. Genomic DNA was isolated from strains that were homozygous for their given mutations for eight generations. B) Time to sterility for *trt-1* single and *trt-1;NHEJ* double mutant strains. Arrows indicate median. C) Telomere erosion in *trt-1* single and *trt-1;cku-80* double mutant strains.

Impact of Ku on telomere shortening in telomerase mutants

Mutation of genes encoding Ku and telomerase genes results in synthetic lethality or rapid telomere shortening in yeast and plants, respectively. (Baumann and Cech, 2000; Heacock et al., 2004; Nugent et al., 1998; Riha and Shippen, 2003). In mice, disruption of Ku causes sterility (Barnes et al., 1998; Samper et al., 2000; Vogel et al., 1999), so synthetic effects of Ku with telomerase were examined in cells derived from mouse strains that had been homozygous for telomerase-deficiency for one or more generations but had been homozygous for Ku-deficiency for only a single generation; no synthetic phenotype was observed (Espejel et al., 2002a). To test whether there is a functional interaction of telomerase with NHEJ components in *C. elegans*, we constructed double mutants defective for telomerase reverse transcriptase *trt-1*, and deletion alleles of three NHEJ components that correspond to Ku70, Ku80, or DNA ligase IV. Upon propagation, *trt-1;cku-70*, *trt-1;cku-80* or *trt-1;lig-4* double mutants reached sterility at similar generations as *trt-1* alone, where the median generation at sterility was 17, 18, 21, and 18, respectively (Figure 2.1B, arrows). Consistent with these observations, Southern analysis using a telomeric probe showed that deficiency for *cku-80* or *lig-4* did not affect the rate of telomere shortening in a *trt-1* background (Figure 2.1C and data not shown). Rates of telomere shortening were 106±27 bp/generation for *trt-1*, 119±15 bp/generation for *trt-1;cku-80,* and 117±46 bp/generation for *trt-1;lig-4* (n=2 strains each), which were not significantly different from one another (P>0.5 in all cases by t-test). Thus, mutation of Ku or DNA ligase IV does not cause synthetic effects in the absence of telomerase in *C. elegans*.

Discussion

In this study, we have demonstrated that disruption of *C. elegans* Ku does not affect telomere length or cause spontaneous telomere uncapping and end-to-end chromosome fusion, phenotypes that have been observed in other systems, but are either controversial or not conserved (Figure 2.1 and data not shown). Furthermore, in a telomerase-deficient background, disruption of Ku did not increase the rate of telomere shortening or cause a synthetic lethal or accelerated senescence phenotype (Figure 2.1).

Studies in *Saccharomyces cerevisiae* yeast and plants indicate that the Ku heterodimer can suppress long 3' overhangs but has variable effects on telomere length. In *S. cerevisiae*, disruption of *YKU70* or *YKU80* causes telomere shortening and constitutive resection of the C-rich strand of telomeric DNA (Bertuch and Lundblad, 2003; Boulton and Jackson, 1996a; Gravel et al., 1998; Maringele and Lydall, 2004; Polotnianka et al., 1998; Porter et al., 1996). In *S. pombe*, disruption of *pku70*$^{+}$ causes short telomeres, rearrangements of telomere associated sequences, and enhanced resection of the C-rich strand during S and G2 phases of the cell cycle (Baumann and Cech, 2000; Kibe et al., 2003; Manolis et al., 2001). In *Kluyveromyces lactis*, disruption of *Ku80* does not alter telomere length but causes elongation of the 3' overhang and increased subtelomeric recombination, indicating that Ku has a capping function in *K. lactis* (Carter et al., 2007). In *Arabidopsis*, disruption of Ku70 or Ku80 leads to extension of the telomere repeat tract and resection of the C-rich strand of telomeric DNA (Gallego et al., 2003; Heacock et al., 2004; Riha and Shippen, 2003; Riha et al., 2002).

Conflicting results have been reported for the effects of Ku and DNA-PKcs at vertebrate telomeres. In Ku-deficient chicken cells, telomeres and telomeric G-overhangs

are normal in length and telomere-telomere fusions are not observed (Wei et al., 2002). Three studies observed that Ku deficiency in mice may cause either telomere shortening (d'Adda di Fagagna et al., 2001) or slight telomere elongation (Espejel et al., 2002a; Samper et al., 2000), whereas telomeric G-strand overhang length is normal (d'Adda di Fagagna et al., 2001; Espejel et al., 2002a; Samper et al., 2000). Several studies show that disrupting mouse Ku causes end-to-end chromosome fusions (Bailey et al., 1999; d'Adda di Fagagna et al., 2001; Difilippantonio et al., 2000; Espejel and Blasco, 2002; Hsu et al., 2000; Samper et al., 2000) that either lack telomeric repeats or contain long telomere tracts at fusion breakpoints (d'Adda di Fagagna et al., 2001; Espejel et al., 2002a; Samper et al., 2000). Suppression of spontaneous end-to-end fusions by mammalian Ku may indicate a 'telomere capping' function distinct from the overhang protection function observed in yeast and *Arabidopsis*. Mice that are mutant for the gene encoding DNA-PKcs have normal telomere length and 3' overhangs and display end-to-end chromosome fusions with long telomere tracts at fusion breakpoints (Bailey et al., 2004; Bailey et al., 1999; Espejel et al., 2002b; Gilley et al., 2001; Goytisolo et al., 2001). Thus, like Ku, the mammalian NHEJ subunit DNA-PKcs helps to cap telomeres. Upon targeted disruption of both copies of human *ku86* in a telomerase-positive somatic cell line, cell death was observed after 8 to 10 population doublings (Li et al., 2002). When heterozygous for *ku86*, these cells exhibit telomere shortening, elongated G-strand overhangs and chromosome fusions (Myung et al., 2004). When Ku86 expression is knocked down by RNA interference in telomerase-positive HeLa cells, a 50% reduction in protein levels caused telomere shortening, chromosome fusions, apoptosis and reduced cell proliferation (Jaco et al., 2004). In contrast, another study found that human cell lines

heterozygous for either *ku86* or *ku70* exhibited moderate telomere elongation and no genome instability (Uegaki et al., 2006). At present, no reports have been published on the effect of DNA-PKcs-deficiency on telomere length in humans. However, two studies have shown that 50% reduction of DNA-PKcs protein levels by RNAi does not cause end-to-end fusions (Zhang et al., 2005; Zhang et al., 2006). In summary, Ku and DNA-PKcs suppress spontaneous end-to-end fusions in mice by a mechanism that is unclear, as no consistent effects on other aspects of telomere metabolism have been reported. Ku may play a more vital role in telomere metabolism in humans, though these data are controversial.

Much species-based variation has also been observed for double deficiency for Ku and telomerase, thereby generating further controversy regarding the relationship between Ku and chromosome termini. In *S. cerevisiae*, double mutants of *est1* or *tlc1* (which are deficient for telomerase in vivo) with *yku70* or *yku80* exhibit synthetic lethality (Nugent et al., 1998). *S. pombe* double mutants for telomerase and Ku exhibit accelerated telomere degradation and senescence compared to telomerase mutants (Baumann and Cech, 2000; Nakamura et al., 1997). In telomerase-deficient *Arabidopsis* plants, disruption of Ku70 hastens telomere shortening and the onset of chromosome fusions (Heacock et al., 2004). In mouse Ku/telomerase double mutants, telomeres shorten at the same rate as those of telomerase mutants, the G-strand overhang is normal, and chromosomes fuse with telomere tracts at the fusion breakpoint, distinct from fusions in telomerase mutants that are devoid of telomere tracts (Espejel et al., 2002a). However, two additional studies have reported distinct phenotypes for mice deficient for both

DNA-PKcs and telomerase: end-to-end fusions either were or were not suppressed by mutation of DNA-PKcs (Espejel et al., 2002b; Maser et al., 2007).

The severe effects of Ku deficiency in yeast or plant telomerase mutants contrast sharply with the lack of such effects in *C. elegans* or mice, suggesting that the role of Ku at telomeres in multicellular animals has been significantly altered, possibly in the context of functional redundancy (Baumann and Cech, 2000; Boulton and Jackson, 1996a; Boulton and Jackson, 1996b; Carter et al., 2007; Riha et al., 2002).

CHAPTER 3

FREQUENCY OF DIRECT END-TO-END CHROMOSOME FUSION EVENTS

Preface

This chapter describes the molecular structures of end-to-end chromosome fusions genetically isolated from telomerase mutants. Three of the mutants described here were isolated by Bettina Meier. I performed linkage analysis and terminal deletion analysis to map fusion breakpoints, PCR to amplify fusion breakpoints, and Southern blotting for physical analysis of fusion breakpoints. The results described here are part of an article that is currently under review at Genetics.

Background and Significance

The natural ends of eukaryotic linear chromosomes present a special challenge for genome integrity: they must be protected from exonucleolytic degradation and must avoid repair by pathways that respond to DNA double-strand breaks. Furthermore, terminal DNA sequences shorten progressively due to the inability of DNA polymerases to replicate the ends of chromosomes and due to processing events that generate 3' overhangs at chromosome termini (reviewed in Lansdorp, 2005; Olovnikov, 1973; Watson, 1972). Protection of chromosome ends is provided by telomeres: DNA-protein complexes typically consisting of short, guanine-rich tandem DNA repeats (TTAGGG in humans) and specific proteins that bind telomeric DNA to promote the integrity and

proper function of telomeres (reviewed in de Lange, 2005). Telomere shortening is offset by telomerase, which adds telomeric DNA repeats to chromosome ends using an RNA template and the telomerase reverse transcriptase (Greider and Blackburn, 1985; Greider and Blackburn, 1987). When cells are deficient for telomerase, their telomeres shorten progressively and eventually become dysfunctional, which can lead to end-to-end chromosome fusion and genomic instability (Harley et al., 1990; Hastie et al., 1990). In addition to telomere length, an important factor in capping is telomere structure, as perturbing telomere binding proteins by altering the telomeric DNA sequence or by expressing dominant-negative telomere binding proteins can lead to end-to-end fusion of telomeres of normal length (Ferreira and Cooper, 2001; Kirk et al., 1997; McEachern and Blackburn, 1995; Miller et al., 2005; Pardo and Marcand, 2005; Prescott and Blackburn, 1997; Underwood et al., 2004; van Steensel et al., 1998).

Given that non-homologous end-joining (NHEJ) ligates DNA sequences that lack homology, this DNA repair pathway may mediate the fusion of uncapped telomeres. Cytological studies indicate that while a core component of the canonical NHEJ machinery is required to fuse acutely uncapped telomeres of normal lengths, disruption of NHEJ does not significantly impair fusion of critically shortened, uncapped telomeres (Maser et al., 2007; Smogorzewska et al., 2002). Other studies rely on PCR to capture transient fusion events that arise as a consequence of telomere erosion, which have revealed DNA sequences for some end-to-end fusion breakpoints (Capper et al., 2007; Cheung et al., 2006; Hackett et al., 2001; Heacock et al., 2004; Hemann et al., 2001; Mieczkowski et al., 2003). These PCR-based studies indicate that NHEJ or microhomology-mediated end-joining (MMEJ) are the major pathways that fuse

uncapped telomeres. However, PCR of genomic template DNA containing end-to-end fusions can bias the fusion events that are recovered. For example, due to limits to product size and molecular structures that are amenable to PCR, large insertions or inverted repeats may have been missed in such assays. In addition, fusion breakpoints that involve exonucleolytic attack of subtelomeric DNA beyond the PCR primer target sites would be missed. Furthermore, PCR primers used in end-to-end fusion experiments typically target only a subset of chromosome ends. Although PCR-based assays have demonstrated that end-to-end fusion can occur as a consequence of direct ligation of uncapped chromosome ends, the frequency of direct ligation events in comparison to the full spectrum of telomeric fusion breakpoint structures has not been quantified in any system.

Mutation of *trt-1*, the *C. elegans* telomerase reverse transcriptase, results in telomere shortening over successive generations, end-to-end chromosome fusions, and progressive sterility (Cheung et al., 2006; Meier et al., 2006). Here, we address the frequency of direct fusion events that arise in *trt-1* mutants, which can be quantified in a relatively unbiased manner in *C. elegans* because its chromosomes are holocentric and thus end-to-end chromosome fusions can be genetically isolated and maintained as stable lines. Our analysis of an unbiased sample of fusion events suggests that direct ligation events favored by PCR assays may not represent the primary mechanism of repair of critically shortened uncapped telomeres.

Materials and Methods

Isolation of end-to-end chromosome fusions

trt-1(ok410),unc-29 or *trt-1(ok410),unc-29;lig-4(tm750)* strains were propagated for multiple generations until brood size had dropped as a consequence of end-to-end fusion. Hermaphrodites from these strains were crossed with wild-type males, and non-Unc F1 L4 hermaphrodites were singled (i.e. transferred to fresh plates, one hermaphrodite per plate). At larval stage L4, hermaphrodites are virgins and singling them ensured that all progeny were self-progeny and not the result of mating with males. F1 that gave rise to a dominant high incidence of males (Him) phenotype in the F2 indicated the presence of an *X*-autosome fusion (Ahmed and Hodgkin, 2000). F2 males from Him F1 were crossed with *unc-1* or *unc-3* hermaphrodites to map the X-linked fusion breakpoint to the left or right end of the *X* chromosome. For each fusion, a total of three outcrosses with *unc-1* or *unc-3* were performed before *X*-autosome fusion homozygotes were isolated. The *unc-29*-linked *trt-1* mutation was removed during these outcrosses.

Complementation and linkage analysis of fusion breakpoints

To determine which autosome ends were involved in the end-to-end chromosome fusions, complementation and linkage analyses were performed. For complementation, fusion strain hermaphrodites were crossed with wild-type males. The resulting male progeny, all carrying an *X*-autosome fusion, were crossed with a hermaphrodite from an independent fusion strain. F1 hermaphrodites were singled and the F2 progeny were scored for the dominant Him phenotype. A Him phenotype indicated complementation

and the presence of *X*-autosome fusions with different breakpoint orientations, whereas a non-Him phenotype indicated that the fusions belonged to the same complementation group. For linkage analysis, the following genetic marker strains were used: *unc-1 X*, *unc-3 X*, *bli-3 I*, *unc-54 I*, *sqt-2 II*, *unc-52 II*, *unc-45 III*, *unc-64 III*, *dpy-9 IV*, *unc-17*, *dpy-20 IV*, *unc-60 V*, and *unc-51 V*. Males carrying an *X*-autosome fusion were crossed with genetic marker hermaphrodites, F1 hermaphrodites were singled, 20 F2 progeny that appeared wild type for the genetic marker mutation were singled, and F3 progeny were scored for the segregation marker phenotype and the dominant Him phenotype, which is tightly linked to each fusion breakpoint. Strains homozygous for a fusion would be non-Him and the lack of marker siblings would indicate linkage.

Molecular analysis of fusion breakpoints

Genomic DNA was prepared using a Puregene DNA Isolation Kit (Gentra). For each fusion strain, all 12 chromosome ends were checked for terminal deletion by PCR using the following subtelomeric primers within the last 1 kb of the telomere.

IL: TCGTCAGCCTTGTTATGTCAACC, GCCTAAGCCTAAAAGAATATGGTAG

IR: TAAGCCTAAGACCAATACCGCAAC, CATTAGGACTGACAGATTGAAAGC

IIL: CATCGCACTTTGAGGACTTTTCC, GCCTAAGCCTAAAATAGTGACTCTG

IIR: ACGCTGTCATCCGAAGCATTGG, GCCTAAGCCTAAAAGCCGCAGC

IIIL: AGTCAGATGGAGGCACGAGTTG, AAAAATAAAATCGGGCTTTTCGACC

IIIR:TGCATTTGTTTTTCCACTTCTGCG,

GGCTTTTCAGATAAAAAAATTGTTTTG

IVL: CAATCAATTTTCGGATTTTTTTTCCC, AAGCCTAAGCCTAAGAAGAGACC

IVR: TTGAAAACTCTGTTTTTTGACGGAG,

CCATTTCTTGTTTTTCTTTCAATAGC

IVR: TCCCATAACCCAAGCCAGTTGC, GCCTAAGCCTAAGCCAGAGAGT

VL: TTTTGAGTTTTTCATTGAGTCGCTG, CATGTCTCTGTACCGACGATATTC

VR: CAATGTATTTTCAATGATTAAAAGCGG, GCCTAAGCCTAAGCAAATCCCC

XL: TTTTCGGAGCTGCAACTTTGTG, CTAAGCCTAAGCCTAATCTGTGC

XR: GCTCTGCTGAATCGACATTTTGC, AATTCTCATTATTCGATAGTAAACCC

PCR assay to detect end-to-end chromosome fusions in late-generation strains deficient for telomerase

Fusion breakpoints were amplified using subtelomeric primers facing telomeres in all pairwise combinations. Optimal PCR conditions were determined by testing primers in pairs that targeted one chromosome end, and primers giving strong, reproducible results were selected to target pairs of chromosome ends.

Physical analysis of fusion breakpoint

Genomic DNA was prepared using a Puregene DNA Isolation Kit (Gentra). DNA was digested with the indicated enzymes and separated on a 0.6% agarose gel at 3.5 *V*/cm. Southern blotting was carried out with a digoxigenin-dUTP-labeled probe following the manufacturer's instructions (Roche) which were made using N2 wild-type genomic DNA as template and the following primers:

ypT27

XR probe: TTGTCAATCTAACCGAACTTATGC, ATGGCGTCACACTTTTCAGG

VL probe: CACTGTGCCATATGGATTCG, TAGCTCTTTTCGAGGCATGG

ypT21

XR probe: TTGATTGAGTAAGGGCTATTTGG, CTGGAAAAATGTGGCAAAGC

IVR probe: TTGCACGGGAAATTTTTATTG, GCACTTCCTTGTAATGCAACC

Results

Isolation of end-to-end chromosome fusions

Molecular analysis of unstable end-to-end fusions from yeast, plants, *C. elegans*, mice and humans has typically relied on PCR using primers adjacent to chromosome ends to amplify fusions from genomic template DNA that contains unknown quantities of end-to-end fusions (Capper et al., 2007; Cheung et al., 2006; Hackett et al., 2001; Heacock et al., 2004; Hemann et al., 2001; Mieczkowski et al., 2003). Although these studies address pathways that process dysfunctional telomeres, the approaches used are biased to recover direct fusions, likely mediated by NHEJ or MMEJ. To test whether direct ligation was the major repair event at critically shortened telomeres, 19 *X*-autosome end-to-end fusions were isolated genetically from independent strains that were homozygous for the telomerase reverse transcriptase deletion mutation *trt-1(ok410)*. Given that dysfunctional telomeres may be substrates of canonical NHEJ, an additional 19 *X*-autosome end-to-end fusions were isolated from *trt-1(ok410);lig-4* double mutant strains that were deficient for the LIG-4 ATP-dependent ligase that is vital for NHEJ-mediated double-strand break repair in *C. elegans* (Clejan et al., 2006; Robert and Bessereau, 2007). The *trt-1* telomerase mutation was separated from each of the 38 fusions that were isolated, and each fusion was outcrossed three times versus a genetic background with wild-type telomeres. All isolated end-to-end chromosome fusions were homozygous viable, indicating that chromosome fusion in the context of telomerase deficiency typically occurs prior to resection that would disrupt essential genes near

uncapped chromosome ends . As a preliminary step towards molecular analysis of the fusion breakpoints, linkage analysis was performed. The breakpoints of each end-to-end fusion were mapped to an end of the *X* chromosome and to an end of an autosome using genetic marker mutations (Figure 3.1A). Complementation tests confirmed the fusion breakpoint map positions, where non-disjunction was not observed for trans-heterozygotes carrying end-to-end fusions with the same *X* and autosome fusion breakpoints . At least one fusion event was recovered for all 12 chromosome ends (Figure 3.1A).

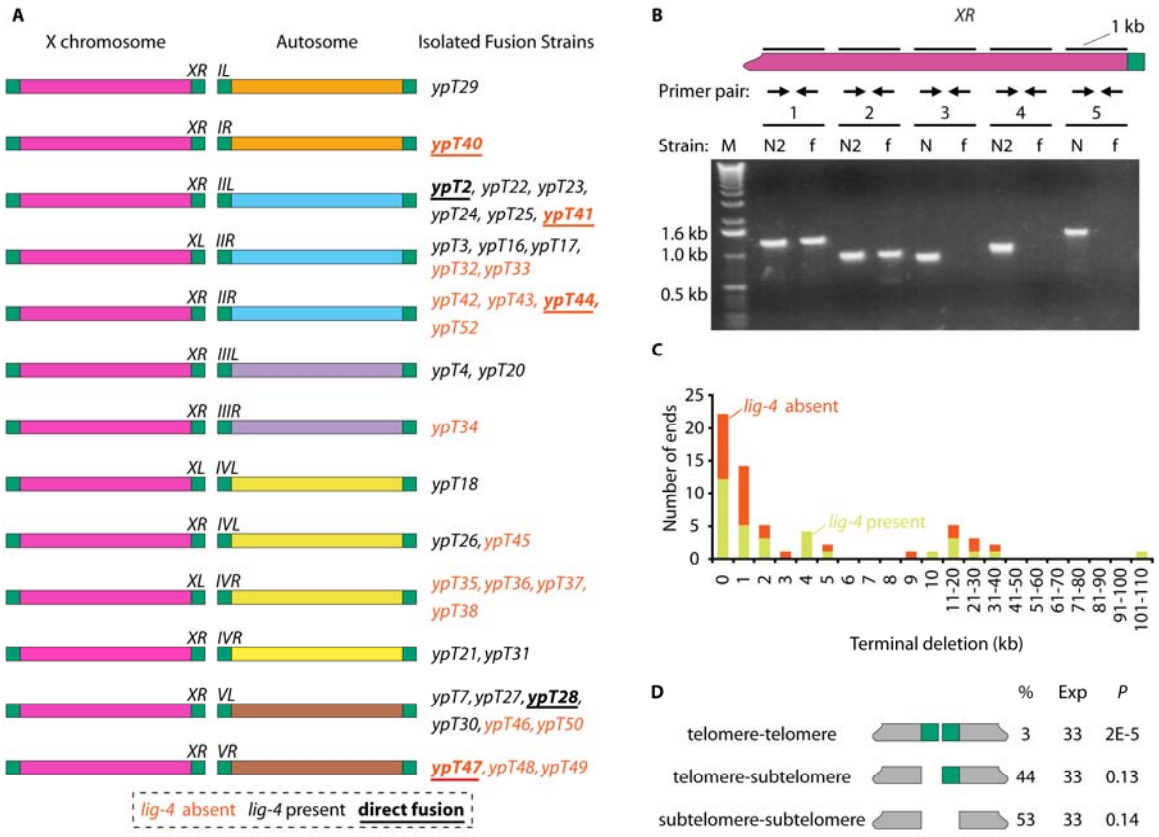

Figure 3.1: Mapping genetically isolated end-to-end chromosome fusion events

A) Fusion breakpoints of 38 *X*-autosome end-to-end fusions, as determined by linkage analysis. Genetic names of each independent fusion are to the right of their fusion orientation. End-to-end fusions that were amenable to PCR are indicated by underlined, bold font. B) Terminal delete analysis to map fusion breakpoints molecularly. PCR results are shown for one chromosome end involved in a fusion. Arrows indicate primers. In this example, one fusion strain was tested with primers targeting 5 kb of subtelomeric DNA. N2: wild-type control. f: *X*-autosome fusion strain. C) Distribution of extent of deletion at chromosome ends. D) Frequency of fusion breakpoint configurations. Observed frequencies (%), expected frequencies (Exp) and *P*-values are shown.

Terminal deletion analysis

Genomic DNA was prepared from each fusion strain and PCR was performed targeting subtelomeric DNA within 1 kb of telomeric tracts at every chromosome end. If a primer pair generated a PCR product using template genomic DNA from N2 wild type but not from a fusion strain, then the targeted region may have been deleted in the fusion strain. Deletions occurred only at chromosome ends that involved a fusion breakpoint (Tables I and II), confirming that outcrossing of each end-to-end fusion had successfully eliminated most unlinked telomeric aberrations that might have been segregating in the telomerase-deficient backgrounds.

Table I. Terminal deletions at X-autosome fusion breakpoints

Strain	Deletion (bp)	
	X chromosome	Autosome
ypT2	2406	5137
ypT28	10230	4364
ypT44	1836	4598
ypT40	994	1261 or 8488[#]
ypT41	954	27627
ypT47	216	314
ypT23	27601	2321

[#]Based on BLAST analysis of the fusion breakpoint sequence, the autosomal deletion breakpoint for *ypT40* occurred at one of two possible sites within a terminal array of rDNA repeats on chromosome *IR* (Wicky et al., 1996)

Breakpoints of those fusions harboring terminal deletions were mapped at 1 kb resolution and then at 5 kb resolution for chromosome ends with more than 5 kb of subtelomeric DNA deleted. In the example in Figure 3.1B, between 2 and 3 kb of

subtelomeric DNA was deleted in the fusion strain, as products were generated for primer pairs 1 and 2, but not for primer pairs 3 to 5. Once an intact region of DNA was found, additional primers were utilized to map the deletion breakpoint at ~500 bp resolution.

Both ends of chromosome *IV* presented difficulty with precise terminal deletion analysis. The subtelomeric sequence abutting the right end of chromosome *IV* (*IVR*) has a tract of DNA composed of 49 copies of a 25-bp direct repeat (Wicky et al., 1996) and is difficult to PCR through (M. Lowden, unpublished data). Thus, terminal deletion analysis at *IVR* relied on primers upstream of the subtelomeric repeats, 1.4 kb from the start of the telomere repeat DNA. The subtelomeric repeats were deleted at one of six *IVR* fusion breakpoints (Table II). Abutting *IVL* is a 23.5 kb inverted repeat (Wilson, 1999). While the spacer between the two copies of the inverted repeat was intact for two of three *IVL* fusion breakpoints, this structure limited further terminal deletion analysis.

Table II. Terminal deletions at X-autosome fusion breakpoints

Strain	Origin	*X* deletion (kb)		Autosome deletion (kb)	
ypT29	*trt-1(ok410)*	*XR*	0.0[#]	*IL*	0.0
ypT22	*trt-1(ok410)*	*XR*	104.7 to 105.3	*IIL*	1.1 to 1.3
ypT24	*trt-1(ok410)*	*XR*	0.0	*IIL*	13.2 to 13.4
ypT25	*trt-1(ok410)*	*XR*	11.0 to 11.4	*IIL*	0.0 to 0.4
ypT16	*trt-1(e2727)*	*XL*	0.0	*IIR*	4.0 to 4.5
ypT3	*trt-1(e2727)*	*XL*	0.0	*IIR*	3.6 to 8.3
ypT17	*trt-1(ok410)*	*XL*	0.0	*IIR*	0.0 to 2.1 kb
ypT32	*trt-1(ok410);lig-4*	*XL*	0.0	*IIR*	10.7 to 11.1
ypT33	*trt-1(ok410);lig-4*	*XL*	0.0	*IIR*	0.0 to 2.1 kb
ypT42	*trt-1(ok410);lig-4*	*XR*	0.2 to 0.5	*IIR*	8.3 to 8.8
ypT43	*trt-1(ok410);lig-4*	*XR*	0.2 to 0.5	*IIR*	10.7 to 11.1
ypT52	*trt-1(ok410);lig-4*	*XR*	20.4 to 20.9	*IIR*	0.0
ypT20	*trt-1(ok410)*	*XL*	0.0	*IIIL*	0.6 to 5.6
ypT4	*trt-1(ok410)*	*XL*	0.0	*IIIL*	0.9 to 1.2
ypT34	*trt-1(ok410);lig-4*	*XL*	0.0 to 0.3	*IIIR*	0.0
ypT18	*trt-1(ok410)*	*XL*	0.0 to 0.3	*IVL*	0.0
ypT26	*trt-1(ok410)*	*XR*	10.4 to 11.0	*IVL*	>47.6
ypT45	*trt-1(ok410);lig-4*	*XR*	30.7 to 31.0	*IVL*	0.0
ypT35	*trt-1(ok410);lig-4*	*XL*	0.0	*IVR*	0.0
ypT36	*trt-1(ok410);lig-4*	*XL*	0.0	*IVR*	0.0
ypT37	*trt-1(ok410);lig-4*	*XL*	0.0	*IVR*	0.0
ypT38	*trt-1(ok410);lig-4*	*XL*	0.0	*IVR*	0.0
ypT21	*trt-1(ok410)*	*XR*	0.8	*IVR*	0.0
ypT31	*trt-1(ok410)*	*XR*	23.9 to 30.7	*IVR*	1.4 to 1.8
ypT7	*trt-1(e2727)*	*XR*	4.2 to 4.4	*VL*	0.0
ypT27	*trt-1(ok410)*	*XR*	0.0	*VL*	4.2 to 4.4
ypT30	*trt-1(ok410)*	*XR*	36.1 to 36.7	*VL*	0.0
ypT46	*trt-1(ok410);lig-4*	*XR*	42.7 to 43.2	*VL*	1.3 to 1.7
ypT50	*trt-1(ok410);lig-4*	*XR*	0.1	*VL*	0.0
ypT48	*trt-1(ok410);lig-4*	*XR*	0.0	*VR*	0.8 to 2.7
ypT49	*trt-1(ok410);lig-4*	*XR*	2.7 to 3.0	*VR*	0.8 to 1.0

[#]0.0 indicates that subtelomeric DNA sequence was intact

Excluding seven *IVL* or *IVR* fusion breakpoints for which no deletion could be detected, 27/69 chromosome ends involved in a fusion event contained telomere repeats. Of 47 chromosome ends with subtelomeric DNA deletions, excluding *ypT40* where the fusion breakpoint could have occurred at two possible sites, 14 were less than 1 kb, 17 were 1 to 5 kb, and 16 were 9 to 105 kb (Figure 3.1C). With respect to terminal deletion analysis, three types of fusion breakpoints occurred: telomere-telomere (3%), telomere-subtelomere (44%), and subtelomere-subtelomere (53%). Telomere-telomere fusions were infrequent, based on the hypothesis that the three configurations were equally likely to occur ($P<2\times10^{-5}$ by t-test) (Figure 3.1D).

All fusion strains containing terminal deletions appeared wild type when homozygous, consistent with the observation that, with one exception, no known genes with visible or lethal phenotypes were disrupted by the terminal deletions (http://www.wormbase.org). The exception is *ypT41*, which carries a 27.6 kb deletion at *IIL* that removes *sqt-2* (SQuaT), which encodes a collagen protein (Kusch and Edgar, 1986). The two alleles of *sqt-2* that have been characterized, *sc3* and *sc108*, each carry a missense mutation that results in *C. elegans* mutants with short fat bodies that are helically twisted so that they roll when they move (Kusch and Edgar, 1986). For all *C. elegans* collagen mutants characterized, a defect in body morphology is caused by point mutations in collagen genes, but no aberrant phenotype occurs for null mutations. Thus, it is not surprising that *ypT41* has no visible phenotype, despite harboring a deletion of *sqt-2*.

PCR of mapped fusion breakpoints

After refining the locations of the deletion breakpoints of end-to-end fusions to within ~500 bp, primers facing each fused chromosome end were utilized to amplify fusion breakpoints. At least two sets of validated primers were tested for each fusion breakpoint. For fusions involving *IVR*, the two *IVR* primers used were as follows: one upstream of the subtelomeric repeats (which may have worked if the subtelomeric repeats were deleted) and one overlapping the subtelomeric and telomeric repeats (which may have worked if *IVR* subtelomeric DNA were intact). No products were amplified for the *IVR* fusions. Fusions involving *IVL* were not tested. Based on PCR analysis, it is unclear whether the fusions of *IVR* or *IVL* were direct. For the remaining 29 fusions whose breakpoints had been clearly mapped, seven yielded PCR products that spanned the fusion breakpoint (Figure 3.1A, underlined and bold). For each fusion breakpoint that was amenable to PCR, terminal deletions occurred at both chromosome ends (Table I and Figure 3.1B). The lack of telomere repeats at direct fusion breakpoints suggests that telomere repeat DNA or telomere binding proteins may repress end-joining in *C. elegans*, as supported by in vitro studies of the mammalian telomere binding proteins RAP1 and TRF2 (Bae and Baumann, 2007).

Sequence analysis demonstrated that all but one of the fusion breakpoints amplified by PCR were simple direct ligations (Table III and Figure 3.1B). For *ypT2* and *ypT28*, isolated from *trt-1*, there was no homology between the X chromosome and the autosome at the fusion breakpoint, suggesting that these fusions may have been mediated by canonical NHEJ (reviewed in Lieber, 1999). Of four end-to-end fusions isolated in the absence of *lig-4*, three (*ypT40*, *ypT41* and *ytT47*) displayed microhomology at the fusion

breakpoints, consistent with observations that MMEJ is a significant end-joining pathway in the absence of the canonical NHEJ machinery (Feldmann et al., 2000; Heacock et al., 2004; Ma et al., 2003; Moore and Haber, 1996; Yu and Gabriel, 2003). The fourth *trt-1;lig-4* fusion breakpoint, *ypT44*, lacked microhomology and occurred in the context of a 4.2 kb inverted repeat normally present at *IIR*, which is flanked by two segments of short tandem DNA repeats, whose repeat sequence is identical (Figure 3.2A). The *IIR* breakpoint occurs within one set of tandem repeats such that the entire inverted repeat is lost and only ~4 of 16 tandem repeats remain. In yeast and mammalian cells, direct and inverted repeats cause genomic instability and are hotspots for mitotic recombination between chromosomes, which can lead to almost complete deletion of the inverted repeat (Lobachev et al., 1998; Lobachev et al., 2000; Waldman et al., 1999). Analogously, the site of the *ypT44* fusion breakpoint may reflect an unusual MMEJ- and *lig-4*-independent mechanism of DSB repair. Finally, the fusion breakpoint of *ypT23*, which had occurred in a strain containing wild-type *lig-4*, had a 410 bp inversion that occurred precisely at its *XR* fusion breakpoint (Figure 3.2B). The inversion is flanked on either side by 1 bp of microhomology, suggestive of MMEJ, though the mechanism by which this inversion occurred is unclear.

Table III. Fusion breakpoints defined in this study. Strains carrying outcrossed homozygous X-autosome fusions are indicated as yp strains. Sequence present at breakpoints is in upper case black font, deleted sequence is in lower case gray font, and microhomology is underlined and bold.

Strain	Origin	Fusion Sequence	
ypT2	*trt-1(ok410)*	*XR*	ACGAGCTTTAtcactaggta
		breakpoint	ACGAGCTTTACATTCACACA
		IIL	ttcccacaacCATTCACACA
ypT28	*trt-1(ok410)*	*XR*	GTTTCAAATCcatggaagcc
		breakpoint	GTTTCAAATCATTCAGTTGT
		VL	atgaggtaatATTCAGTTGT
not isolated[#]	*trt-1(ok410).a generation F10*	*IIR*	TTTGTCAAAAatccaatttc
		breakpoint	TTTGTCAAAAGTACCGACGA
		VL	tcatgtctctGTACCGACGA
ypT44	*trt-1(ok410);lig-4*	*XR*	GTATATTTTTtcagtacatg
		breakpoint	GTATATTTTTCCCAGCTTCA
		IIR	gatacagaacCCCAGCTTCA
ypT40	*trt-1(ok410);lig-4*	*XR*	CATTTT**GCTA**atttttaaa
		breakpoint	CATTTT**GCTA**CCTTGTTACG
		IR	cctaca**GCTA**CCTTGTTACG
ypT41	*trt-1(ok410);lig-4*	*XR*	ACCCAAG**CTT**tgccacattt
		breakpoint	ACCCAAG**CTT**CATGTTGGAA
		IIL	tttgaca**CTT**CATGTTGGAA
ypT47	*trt-1(ok410);lig-4*	*XR*	GTGCAC**GGAG**tcgagaaacc
		breakpoint	GTGCAC**GGAG**GTTTTTAAAG
		VR	tttaca**GGAG**GTTTTTAAAG

[#]Non-outcrossed fusion recovered by PCR using template genomic DNA from a telomerase mutant harboring end-to-end chromosome fusions

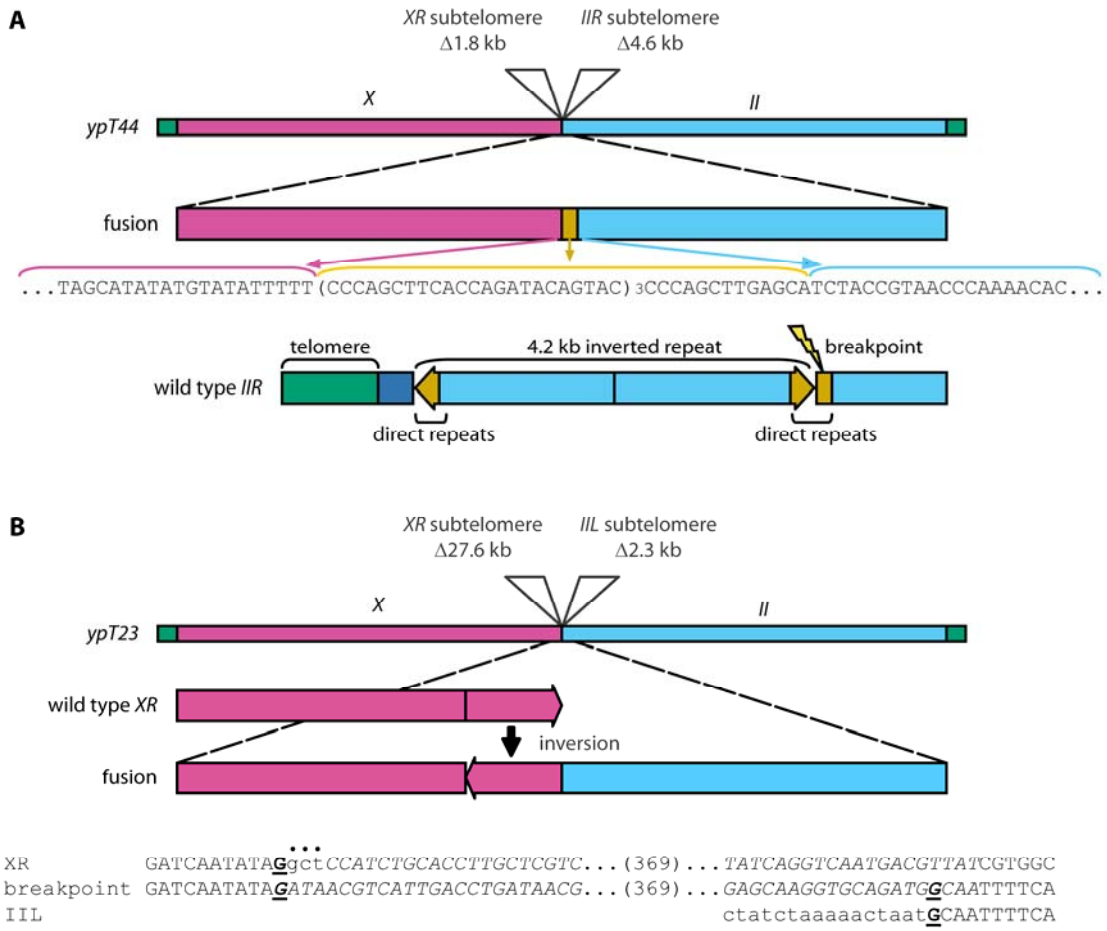

Figure 3.2: Fusion breakpoint structures of two direct fusions

A) The drawing depicts the fusion breakpoint for *ypT44*. Sequencing shows that some subtelomeric direct repeats remain intact. Below the breakpoint sequence is the structure of inverted repeats and direct repeats at wild-type *IIR*. B) An inversion at the fusion breakpoint of *ypT23* is shown. A 3 bp deletion occurred at the inversion, denoted by a dot above the breakpoint sequence. Bold and underlined font indicates microhomology at the breakpoints.

In summary, despite careful genetic and molecular mapping of 29 fusion breakpoints, only 7 were amplified, 6 of which were direct ligations and one of which contained a small inversion. Thus, our results indicate that direct ligation may not be the major pathway for the genesis of end-to-end fusions that occur as a consequence of telomere attrition.

PCR of unmapped fusion breakpoints

To confirm our observations that the frequency of direct fusion was low, we utilized an approach similar to previous PCR-based studies performed in other organisms. Genomic template DNA from mid- to late-generation *C. elegans* telomere replication mutant strains that had accumulated end-to-end fusions was analyzed using a PCR-based strategy that examines almost all possible permutations that could result from end-to-end fusion of *C. elegans* chromosomes. The haploid number of chromosomes in *C. elegans* is six. Although some regions of subtelomeric DNA are repeated at internal genomic sites, the subtelomeric sequences at each chromosome end differ from one another and possess unique primer targets (http://www.wormbase.org, Wicky et al., 1996). Fifty pairwise combinations of subtelomeric primers were utilized to encompass every possible fusion event between different chromosomes, excluding *IVR* (see above). To test whether PCR could amplify fusion breakpoints from late-generation telomere replication-defective strains that may have accumulated multiple fusions, controls were performed with pooled genomic DNA from wild type and from six isolated *X*-autosome fusion strains (Figure 3.3) where direct ligation of chromosome ends had occurred (such that DNA from each fusion strain was diluted 1:9). Under these conditions of non-homogeneous template genomic DNA, mapped fusions breakpoints were amplified robustly and consistently .

Additional controls were performed to test primers targeting 11 chromosome ends (excluding *IVR*), individually and in pairs, to ensure that all the primers worked effectively and specifically under the same reaction conditions. Once appropriate primers and conditions were selected, the following telomere replication mutants were analyzed for fusion breakpoints: *trt-1* or *mrt-2* single mutants, and four double mutants: *trt-1;mrt-2*, *trt-1;cku-80(ok861)*, *trt-1;lig-4(ok416)*, and *trt-1;lig-4(tm750)* (n=28 mid- to late-generation telomere replication-defective strains). *mrt-2* encodes a subunit of the 9-1-1 DNA damage response complex that is required for telomerase activity in vivo (Ahmed and Hodgkin, 2000; Meier et al., 2006). Strains were subjected to a population bottleneck of six individuals every two generations and passaged until every animal contained multiple fusions, some of which might have been shared based on common ancestry, prior to preparation of genomic DNA for PCR analysis. In an exhaustive attempt to amplify fusion breakpoints, each chromosome end was targeted by one primer within 2 kb of the telomeric tract, which mimics other PCR-based end-to-end fusion assays where primers are usually targeted within 1 kb of telomere repeat tracts. A total of 50 primer pairs tested on 28 telomere replication mutant strains. Although weak bands were occasionally observed, none were reproducible, and no fusion breakpoints were amplified (Figure 3.3A).

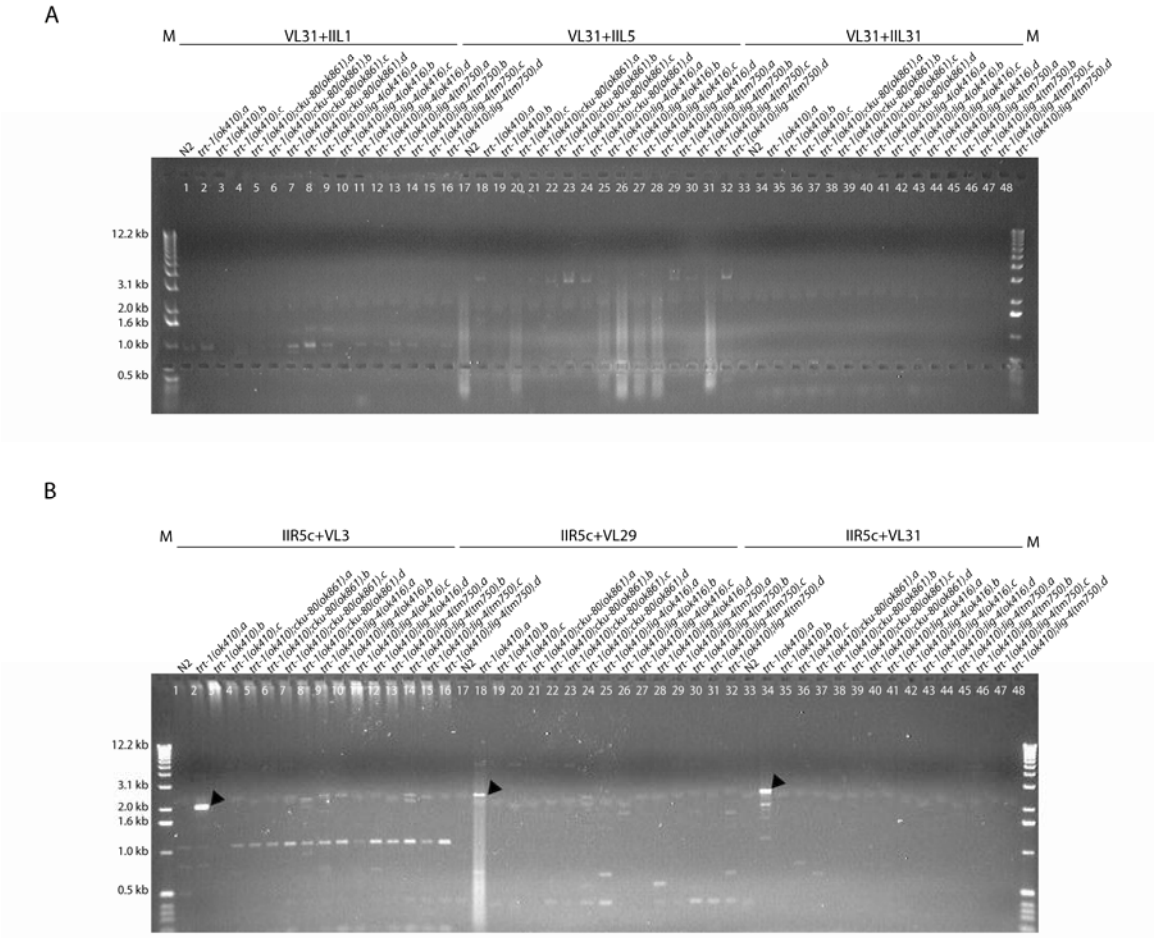

Figure 3.3: PCR amplification of end-to-end fusions from telomerase mutants. Three primer pairs were utilized on 16 strains, including the wild-type contol, as indicated. M: 1 kb ladder (Invitrogen). A) PCR targeting *IIR* and *VL*. All of the PCR reactions containing genomic DNA from telomerase-deficient strains displayed non-specific, weak bands or smears. B) PCR targeting *IIL* and *VL*. Arrowheads indicate PCR products for one strain, *trt-1(ok410).a* for all three primer pairs. While all three reactions contained the same primer targeting *IIR* each reaction contained a different primer targeting *VL* at sites 1371 bp 1651 bp and 1768 bp from the start of the telomere repeats for VL3 VL29, and VL31 respectively.

In agreement with our poor success at amplifying unmapped fusion breakpoints using primers that target the terminal 2 kb of subtelomeric DNA, deletions of 2 kb typically occurred at one or both chromosome ends for genetically isolated end-to-end fusions where direct ligation had occurred (Table I). In addition, most of the isolated *X*-autosome fusion strains harbored fusion events involving chromosomes *II* and *V* (Figure 3.2A). Accordingly, PCR reactions using template DNA from each of the individual mid- to late-generation telomere replication strains were performed using 24 primer pairs 1 to 5 kb away from the telomere tracts of chromosomes *II* and *V*. Three reactions amplified a fusion breakpoint for one *trt-1* strain, whose PCR product sizes were consistent with the amplification of the same fusion breakpoint (Figure 3.3B). Sequencing of those PCR products revealed a fusion breakpoint that contained deletions of 2,229 and 112 bp at *IIR* and *VL*, respectively, and displayed no microhomology. The lack of microhomology indicates that this fusion event probably arose as a consequence of canonical NHEJ, in agreement with the two breakpoints from genetically isolated fusions derived from *trt-1* strains with wild-type *lig-4* (Table III). Thus, we recovered a single autosome-autosome fusion event from genomic DNA of 28 strains that each harbored multiple end-to-end fusions.

Taken together, analysis of genetically isolated end-to-end fusions whose breakpoints were precisely mapped, as well as PCR-based analysis of non-outcrossed, unmapped fusions of mid- to late-generation telomere replication mutant strains, revealed that end-to-end fusions typically do not occur as a consequence of simple end-joining. Under our conditions, the maximum size of the PCR products that could be amplified from *C. elegans* genomic DNA was 11 kb. Thus, the remaining fusion breakpoints may

involve genome duplications greater than 11 kb in length. An alternative possibility is that all fusion breakpoints occurred as a consequence of direct ligation of uncapped chromosome ends, but that PCR failed at these fusion breakpoints due to the presence of DNA sequences that are not amenable to PCR. To distinguish between these possibilities, Southern blotting was performed.

Physical analysis of fusion breakpoints

By using genetically isolated end-to-end fusions, large quantities of DNA from many animals homozygous for a single fusion event can be obtained, which allows for physical analysis by Southern blotting. To examine the physical structure of fusion breakpoints that were refractory to PCR, genomic DNA isolated from fusion strains *ypT21* and *ypT27* was subjected to Southern analysis using probes designed to hybridize to either side of their mapped fusion breakpoints. The genomic DNA for each strain was digested with restriction enzymes to produce restriction fragments of various sizes at each fusion breakpoint. If the fusion events occurred as a consequence of direct ligation, then flanking probes ought to detect a single fusion breakpoint restriction fragment. Alternatively, detection of restriction fragments of different sizes would indicate that an insertion of DNA containing additional restriction sites had occurred at a fusion breakpoint. For strain *ypT27*, which carries a *XR*-*VL* fusion, probes targeting *XR* and *VL* hybridized to different restriction fragments: *Ava*II, 1.7 kb and 3.2 kb fragments, respectively; *Hin*dIII, 1.3 kb and 5.2 kb fragments, respectively; and *Pfl*MI, 2.9 kb and 2.4 kb fragments, respectively (Figure 3.4A-B). For *ypT21*, an *XR*-*IVR* fusion, genomic DNA digested with *Hpa*II, the *XR* and *IVR* probes hybridized to 2.4 kb and 3.5 kb fragments, respectively (Figure 3.4D-F). For *ypT21* digested with *Pml*I, the results were

ambiguous because the *XR* probe hybridized to multiple fragments and showed the same pattern as wild type. Nevertheless, the *HpaII* data clearly support the conclusion that there is an insertion containing additional restriction sites at the fusion breakpoint of *ypT21*. The probes used to analyze the fusion breakpoints for *ypT27* or *ypT21* detected the predicted restriction fragments of wild-type genomic DNA, confirming that the probes were targeting the correct restriction fragments (Figure 3.4). Thus, physical analysis supports the interpretation that fusion breakpoints that are refractory to PCR do not occur as a consequence of direct ligation, but instead represent complex DNA repair events that result in duplication of one or more segments of the genome at a fusion breakpoint.

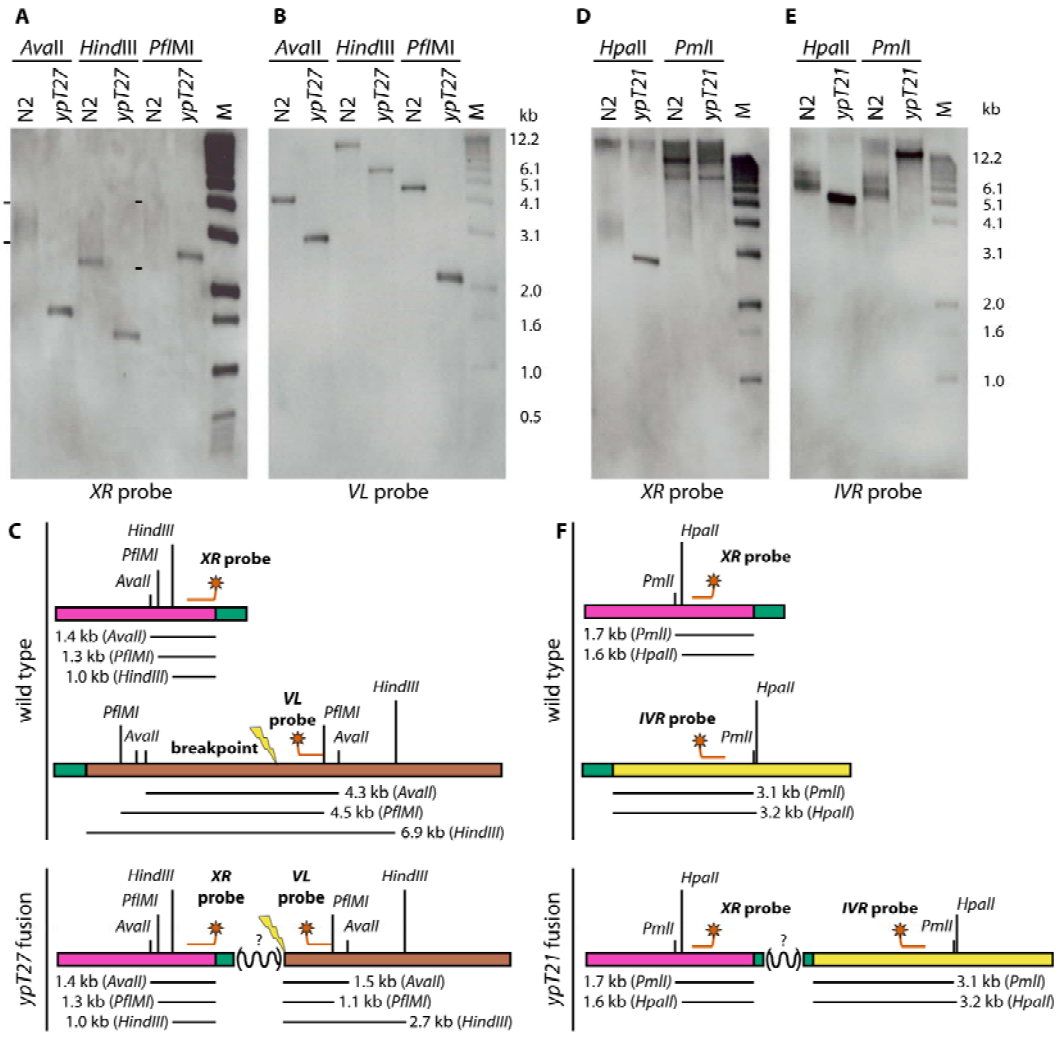

Figure 3.4: Southern analysis of fusion breakpoints that were refractory to PCR. Wild-type and mutant DNA digests using the enzymes indicated are shown. A) *ypT27* fusion breakpoint was probed with *XR* and B) *VL* subtelomeric probes. Wild-type signals were as predicted: >1.4 kb, >1.3 kb, and >1.0 kb (*XR*) and 4.3 kb, 4.5 kb, and >7.2 kb (*VL*) for *Ava*II, *Hind*III or *PflM*I, respectively. The bounds of the smeary signals associated with terminal restriction fragments (containing telomeric DNA) are indicated by dashes to the left of a given lane. C) The restriction fragments predicted to be detected by each probe for wild type and *ypT27* are shown. D) *ypT21* was probed with *XR* and (E)

IVR subtelomeric probes. Wild type signals were as predicted: >1.6 kb and >1.7 kb (*XR*) or >3.2 kb and >3.1 kb (*IVR*) for *Hpa*II and *Pml*I, respectively. F) The restriction fragments predicted to be detected by each probe for wild type and *ypT21* are shown.

Discussion

Here, we have demonstrated that *C. elegans* telomere replication mutants can accumulate end-to-end fusions in the absence of DNA ligase IV. Our findings are in strong agreement with studies that show DNA ligase IV is not required for end-to-end fusion of critically shortened telomeres in telomerase mutants in *S. cerevisiae*, *S. pombe*, *Arabidopsis*, or mice (Baumann and Cech, 2000; Hackett et al., 2001; Heacock et al., 2004; Maser et al., 2007). In contrast, end-to-end fusion of uncapped telomeres of normal length in *S. cerevisiae*, *S. pombe* and *K. lactis* and mice depends on DNA ligase IV (Carter et al., 2007; Ferreira and Cooper, 2001; Mieczkowski et al., 2003; Pardo and Marcand, 2005; Smogorzewska et al., 2002). Thus, processing and fusion of acutely uncapped long telomeres can rely on a specific DNA repair pathway (canonical NHEJ), whereas fusion of telomeres that shorten progressively in the absence of telomerase may be a more promiscuous process that can occur via several DNA repair pathways (reviewed in Riha et al., 2006).

Molecular analyses of dysfunctional telomeres in yeast, plants, worms, mice and humans reveal that end-to-end fusion can be mediated by direct ligation of uncapped telomeres (Capper et al., 2007; Cheung et al., 2006; Hackett et al., 2001; Heacock et al., 2004; Hemann et al., 2001; Mieczkowski et al., 2003). However, the frequency of directly ligated fusion breakpoints could not be determined in these studies, which would miss 1) direct fusion events that involve extensive terminal deletions, or 2) complex fusion breakpoints with insertions of large segments of DNA. The holocentric chromosomes of *C. elegans* result in stable end-to-end fusions where an unbiased collection of fusion events can be outcrossed and recovered for quantitative analysis in a

manner that is not possible in most model systems. We found that direct fusion events at critically shortened telomeres occur infrequently (Figure 3.1A and Table III). In a parallel approach resembling PCR-based experiments conducted in other systems, PCR primers at 11 out of 12 chromosome ends failed to reveal significant levels of direct end-to-end fusions in genomic DNA from 28 strains harboring end-to-end fusions. Thus, independent approaches indicate that direct ligation does not explain the majority of DNA repair events at critically shortened telomeres.

How, then, do the majority of end-to-end chromosome fusions arise? Southern analysis of genetically isolated end-to-end fusions revealed that probes flanking fusion breakpoints that were refractory to PCR detected restriction fragments of different sizes, whereas a single fusion breakpoint restriction fragment would have been detected for a direct ligation event (Figure 3.4). Thus, many fusion breakpoints that arise when telomerase is deficient may contain insertions of large segments of genomic DNA. In human cells, end-to-end chromosome fusion results in dicentric chromosomes that often break during anaphase and subsequently form new fusions, which impedes analysis of their fusion breakpoints (reviewed in Bailey and Murnane, 2006). Either these fusion events or the ensuing genomic instability associated with breakage-fusion-bridge cycles (McClintock, 1941) may promote tumorigenesis (Murnane and Sabatier, 2004). Our results suggest that end-to-end chromosome fusion breakpoints that arise when telomerase is deficient may represent complex recombination events.

Studies in other systems are consistent with our observations. Molecular and genetic analyses of telomerase-deficient yeast mutants reveal that dysfunctional telomeres can copy large segments of DNA from an intact chromosome end via break-

induced replication (Hackett et al., 2001). End-to-end fusion and recombination between sister chromatids occurs at dysfunctional telomeres in mammalian cells and can generate duplications at chromosome ends, as shown in cytological studies (reviewed in Bailey and Murnane, 2006). Furthermore, a complex fusion breakpoint involving a small duplication of one chromosome end was recovered by PCR in the context of telomerase deficiency in *Arabidopsis*, an observation that agrees with cytogenetic measurements of fusion between homologous chromosomes or sister chromatids (Heacock et al., 2004; Siroky et al., 2003). Sister chromatid recombination events also have been observed in *C. elegans* using template genomic DNA from *trt-1* mutants and a PCR primer that targets a single chromosome end (Cheung et al., 2006). Together, the latter observations suggest that alternatives to direct end-to-end fusion exist. Thus, the low frequency of direct fusion events observed for end-to-end chromosome fusions genetically isolated from *C. elegans*, as well as in genomic DNA from late-generation telomerase mutants, may be broadly relevant.

We conclude that the majority of end-to-end fusions that occur as a consequence of telomere erosion may be fundamentally different in nature from the direct fusion events that can be detected by PCR-based analysis of heterogeneous mixtures of genomic DNA harboring end-to-end fusions. The structures of complex fusion breakpoints isolated from *C. elegans* telomerase mutants are currently under investigation and are the topic of Chapter 4.

CHAPTER 4

MOLECULAR STRUCTURE OF COMPLEX END-TO-END FUSION EVENTS

Preface

This chapter describes the molecular structures of complex fusion breakpoints that could not be amplified by PCR using primers at each fused chromosome end. I carried out inverse PCR analysis and prepared DNA for microarray analysis. Stephane Flibotte a faculty member at University of British Columbia in Vancouver, BC, Canada designed the microarray and analyzed the raw data to determine the $\log_2$(fusion/wild type signal). Probe preparation and hybridization and scanning of the microarray were done by NimbleGen. The work described here is ongoing and has not yet been submitted for publication.

Background and Significance

Metaphase spreads reveal at a glance the dramatic chromosomal aberrations that can occur in tumor cells. The underlying mechanisms driving these aberrations are largely unknown. Molecular details of chromosomal rearrangements may explain the phenotypic diversity among tumors. For example, changes in DNA copy number may contribute to changes in mRNA expression that contribute to the difference between a fast-growing 'basal-like' tumor associated with a high mortality rate and a 'luminal A' tumor that has a good prognosis (Perou et al., 2000; Pollack et al., 2002). Thus, understanding the

mechanisms underlying alterations to tumor genomes may help in diagnosis or treatment of cancer.

Cancer incidence increases and telomere length decreases with age. In cultured cells, critically shortened telomeres are responsible for the phenomenon of crisis, where end-to-end fusions accumulate and most cells die. One or more fusion events may promote escape from crisis and oncogenesis, perhaps by activation of telomerase or ALT. Stable end-to-end fusion events in *C. elegans* provide a unique opportunity to investigate the structures that arise upon fusion of critically shortened telomeres. While some fusion events isolated from *C. elegans* telomerase mutants were direct ligation events, others contained duplications and may be analogous to the complex aberrations that can occur in tumor cells. To investigate the molecular structures of complex end-to-end fusion events isolated from *C. elegans* telomerase mutants, inverse PCR was used to gain information about fusion breakpoints that had been refractory to direct PCR with primers targeting fused chromosome ends. Sequencing inverse PCR products revealed insertions at some fusion breakpoints which were too large to be defined by further PCR analysis. Microarray analysis to look for changes in DNA copy number confirmed duplications that were predicted by inverse PCR, and, intriguingly, revealed a significant degree of complexity to the DNA repair events that create end-to-end fusions. Preliminary results for this phase of my project are described here.

Materials and Methods

Inverse PCR

Genomic DNA was prepared using a Puregene DNA Isolation Kit (Gentra). DNA was digested with *Sca*I, *Rsa*I. Digested DNA was purified and then subjected to ligation

by T4 DNA ligase (New England Biolabs). Ligations were purified and then used as templates in PCR reactions. After one round of PCR, products were purified and subjected to a second round of PCR.

Microarray analysis

Worms were grown on NGM agarose glucose plates until starvation, harvested from plates, washed 7 times, returned to fresh plates overnight, harvested again and then frozen. Subsequently, genomic DNA was prepared using a Puregene DNA Isolation Kit (Gentra). This treatment ensured that little or no bacteria remained on the worms or in their guts, and thus bacterial DNA would not interfere with microarray analysis. Genomic DNA was fragmented and labeled by NimbleGen as follows. Genomic DNA was sonicated and an aliquot was run on a gel to confirm that fragments were between 500 and 2000 bp. Fusion DNA samples were labeled with Cy3 and the wild type DNA sample was labeled with Cy5 by amplifying genomic DNA with Klenow and dye-labeled random 9-mers (TriLink BioTechnologies, Inc.) Labeled DNA was purified by isopropanol precipitation and DNA concentration was measured using a spectrophotometer. Samples were hybridized in the NimbleGen Service Facility. Labeled fusion and wild type DNA

samples were combined and were hybridized to a microarray. The microarray was washed with NimbleGen wash buffers and scanned on an Axon scanner (Model # 4000B).

Results

Inverse PCR

As presented in Chapter 3, Southern blotting revealed that insertions occurred at two fusion breakpoints that were refractory to PCR. To identify the duplicated sequences, inverse PCR was performed as follows: genomic DNA was digested with a restriction enzyme that cuts near the fusion breakpoint, ligated under conditions that favor circularization, and PCR-amplified with primers that targeted one chromosome and faced away from each other (Figure 4.1A). Using this strategy, an insertion at the fusion breakpoint may be cut into a fragment that is amenable to PCR and subsequently can be sequenced. Controls to amplify circularized templates that did not contain fusion breakpoints were successful using wild type or fusion genomic DNA, whose products ranged in size from 0.1 to 6.2 kb .

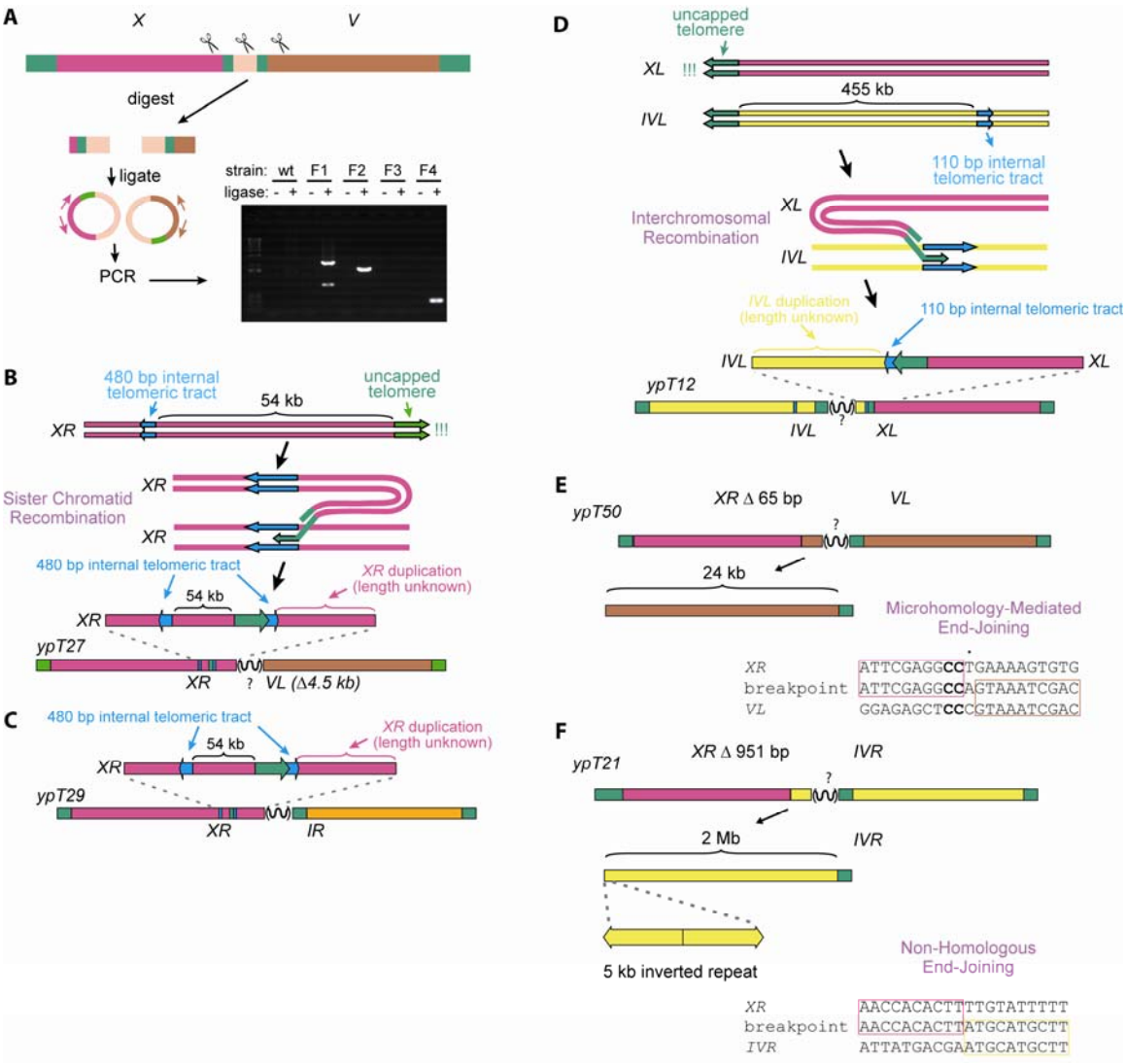

Figure 4.1: Inverse PCR to amplify fusion breakpoints. A) Inverse PCR using template genomic DNA from wild type and from four fusion strains (F1, F2, F3, F4) revealed fusion-specific PCR products. Inverse PCR at the *X* chromosome fusion breakpoint revealed recombination of an uncapped telomere and an internal telomeric tract at *XR* for (B) *ypT27* and (C) *ypT29* or (D) at *IVL* for *ypT12*. Duplications mediated by direct ligation occurred for (E) *ypT50* and (F) *ypT21*. Bold font and dot indicate microhomology and insertion, respectively.

Since 12 fusion breakpoints occurred within 1 kb of the telomeric repeat tracts at *XR*, they were tested using the same restriction enzyme (*Sca*I) and nested primer pairs. PCR products were made for 8/12 fusion breakpoints. Two fusion breakpoints gave smeary products that were unsuitable for sequencing. Three direct fusion events were included in the inverse PCR analysis, and all made products. Four fusion breakpoints showed clear evidence for insertions, while two remaining fusion breakpoints were less clear. The latter two sets of fusion breakpoints are described in detail below. An additional fusion breakpoint was recovered in an inverse PCR experiment targeting 13 *XL* fusion breakpoints. In wild type, a 10 kb inverted repeat abuts the telomere at *XL*. Although one primer used for inverse PCR should have specifically targeted the terminal copy of the inverted repeat since the final two nucleotides at the 3' end of the primer were unique, all *XL* fusions produced the same product as wild type for inverse PCR with one enzyme and no product for a second enzyme. For the sole exception, a unique PCR product was amplified.

Insertions occurred at 5 fusion breakpoints that were consistent with either recombination between telomere and internal telomeric sequences or NHEJ (Figure 4.1B-F). For *ypT27* and *ypT29*, recombination occurred between the *XR* telomere and an internal telomeric sequence tract 54 kb from the *XR* telomere, likely as a result of sister chromatid recombination (Figure 4.1B,C). Since the recombination event went towards *XL*, the extent of the insertion is not clear, but most likely the duplication does not extend all the way to *XL* as this might cause the same phenotype as an animal carrying three copies of the X chromosomes, dumpy (short fat) body morphology (Hodgkin et al., 1979). For *ypT27*, the inverse PCR product captured an initial recombination event with

an internal telomeric sequence which was followed by an inversion event 2 to 3 kb away. For *ypT12*, recombination occurred between the *XL* telomere an internal telomeric sequence tract 455 kb from *IVL* (Figure 4.1D). This recombination event went toward IVR, suggesting that the fusion breakpoint has a 455 kb deletion of *IVL*. However, this is not consistent with terminal deletion analysis at *IVL* and a 455 kb deletion would remove genes known to cause lethal and visible phenotypes (e.g. *dpy-9*, *spl-1*, and *rps-1*).The extent of the insertion is not clear. Since trisomy for chromosome *IV* does not cause lethality or other visible phenotypes, an upper limit for the insertion cannot be predicted (Herman and Kari, 1989). A 24 kb insertion *VL* occurred at the fusion breakpoint of *ypT50*, an *XR-VL* fusion (Figure 4.1E). The insertion starts 24 kb from the telomeric repeat tract of *VL* and moves toward *VL*. The breakpoint exhibits 3 bp of microhomology, consistent with direct ligation events isolated from *trt-1;lig-4* double mutants (Chapter 3). The inverse PCR product for *ypT21*, an *XR-IVR* fusion, reveals that *XR* had a terminal deletion of 951 bp and was fused to a site 2.1 Mb from the *IVR* telomere within an inverted repeat (Figure 4.1F). Thus, the orientation of the insertion is not clear. However, as a 2.1 Mb deletion would be lethal, it is likely that a 2.1 Mb duplication occurred. The fusion breakpoint exhibits no microhomology, consistent with direct ligation events isolated from *trt-1* mutants with wild-type *lig-4*. Thus, HR, MMEJ, or NHEJ may all act to repair uncapped telomeres.

Sequencing of the inverse PCR products for two fusion events gave unclear results. For *ypT42* and *eT3*, the PCR products were smaller than the expected minimum product sizes. The expected and observed product sizes were 0.5 versus 0.3 kb (*ypT42*) and 0.6 versus 0.3 kb (*eT3*). The orientation of the DNA sequences did not indicate that

inversions occurred. However, sequencing only worked with the primer facing the ligation site, and not with the primer facing the fusion breakpoint. Furthermore for *ypT42*, the sequence was consistent with a 0.9 kb deletion at *XR*, in disagreement with terminal deletion analysis which indicated a 0.2 to 0.5 kb deletion. Similarly, terminal deletion analysis shows that *XR* is intact for *eT3*, but the inverse PCR product sequence is consistent 0.2 kb deletion. Perhaps a rearrangement occurred for both of these fusion events, but the details are unclear.

Inverse PCR was useful to confirm that insertions occurred at some fusion breakpoints, however, this method provides limited information. Comparative genomic hybridization (CGH) microarray analysis could show the extent of an insertion. In 5/5 cases, insertions at the fusion breakpoint involved one of the chromosome ends shown by linkage analysis to be involved in the fusion event. But it's possible that while inverse PCR captures only a small part of an insertion, the global view provided by CGH microarrays could reveal copy number changes at chromosome ends that have been implicated in the fusion event.

Microarray Comparative Genomic Hybridization

Recently, the first study of CGH microarray analysis in *C. elegans* was published by the research group of Dr. Donald Moerman (Maydan et al., 2007). The paper especially stood out because of the high resolution of the microarray. Our initial attempts at microarray CGH failed because the array did not have sufficient resolution. However, in collaboration with the Moerman lab, a chip was designed specifically for analysis of the fusion strains. The coverage was fairly uniform across the genome, with extra coverage in the terminal 2 Mb of each chromosome end (where duplications might be

expected) and even more coverage in the last 5 kb (where many deletions occurred), as well as at 1 kb regions flanking all mapped fusion breakpoints that occurred more than 5 kb from telomeres. This design should allow all of the fusion breakpoints to be analyzed using the same array design, which may help to remove bias or artifacts that may occur as a consequence of the array itself or of the genetic backgrounds from which the chromosome fusions were derived.

In a pilot experiment, three *X*-autosome fusion strains were tested: *ypT41*, *ypT21*, and *ypT27*. *ypT41* (*XR*-*IIL*) was a control fusion strain where a direct end-to-end fusion event and the accompanying terminal deletions were the only predicted changes to the genome. Inverse PCR for *ypT21* (*XR*-*IVR*) targeting *XR* indicated that *XR* had a terminal deletion of 796 bp and may have contained a 2 Mb insertion of *IVR* mediated by NHEJ. Terminal deletion analysis at *IVR* was limited by subtelomeric direct repeats that abut the telomere and impeded PCR. Thus, *ypT21* has either no terminal deletion at *IVR* or a deletion less than 1.4 kb. Inverse PCR for *ypT27* (*XR*-*VL*) indicated that *XR* was intact and its telomere recombined with an internal telomeric sequence that is normally present 54 kb from the *XR* telomere. The duplication is at least 5 kb and could have involved a significant portion of the *X* chromosome. Terminal deletion analysis indicated that *VL* has a 4.4 to 4.6 kb deletion.

For the control direct fusion event, *ypT41*, microarray analysis agreed with sequencing data that revealed terminal deletion of 954 bp and 27627 bp at *XR* and *IIL*, respectively. No other copy number changes occurred, except for a deletion at *IVR*, which may have been in the genetic background, as it appeared for *ypT27* as well.

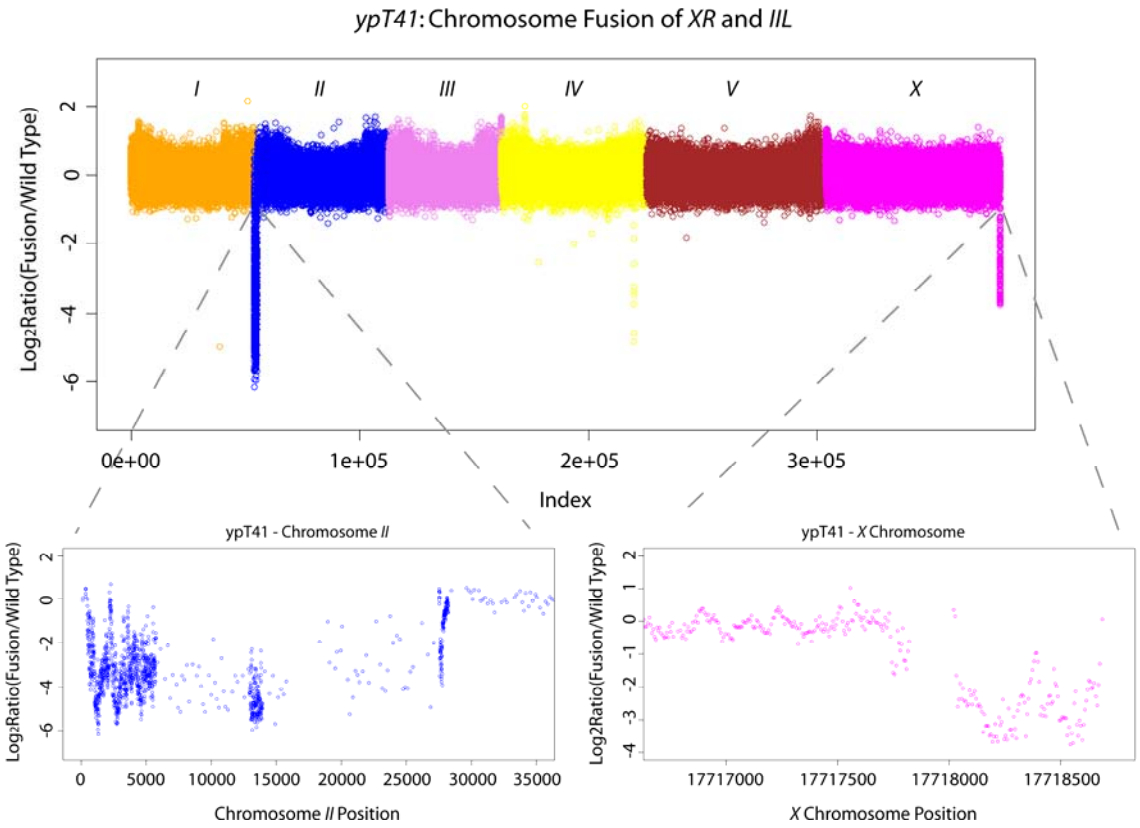

Figure 4.2: Microarray CGH data for ypT41. The Y-axis represents the ratio of array signal intensity for fusion versus wild type, where a negative ratio indicates a decrease in fusion copy number. Lone circles represent noise. Strong peaks are clusters of adjacent oligos with altered copy number. The X-axis scale is non-linear due to non-uniform oligo density on the arrays, which results in slight smiles in the middle of each chromosome.

Microarray analysis of *ypT27* revealed an expected terminal deletion at *VL*, as well as the extent of genome duplication associated with recombination between an unapped telomere and an internal telomeric tract. Based on inverse PCR, we anticipated a duplication starting 54 kb from *XR* and moving toward *XL*, but, surprisingly, the terminal 61 kb of *XR* were duplicated instead, which was associated with a triplication event immediately to the left of the initial recombination event. While a $\log_2$(fusion/wild type) with an amplitude of 0 indicates no copy number change and an amplitude of 1 indicates a duplication in the fusion DNA, an amplitude of 1.6 would indicate a triplication. A signal of 1.6 or greater occurred 61 kb from *XR* and spanned 10 kb. The precise sequence of this amplification event is not clear based on microarray analysis alone, although PCR and sequencing may confirm how it occurred.

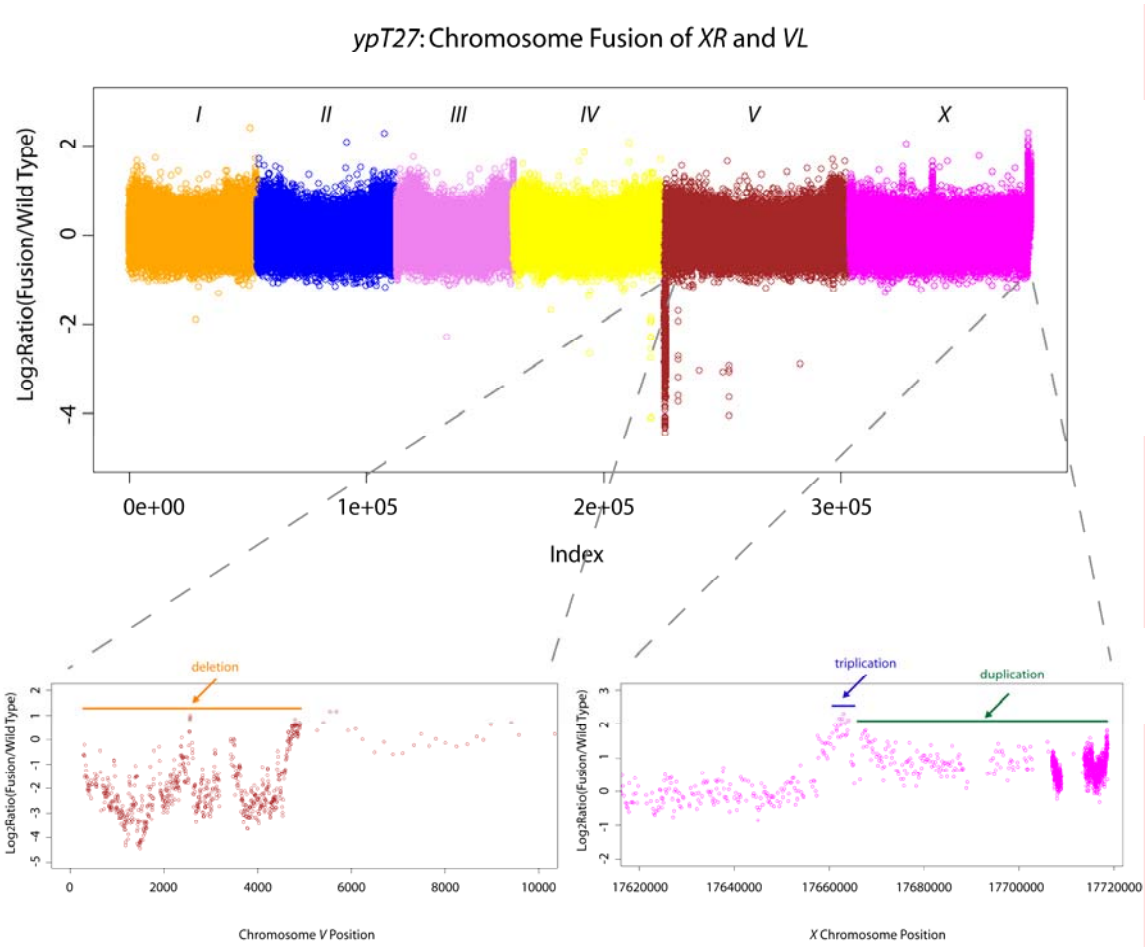

Figure 4.3: Microarray CGH data for ypT27. The Y-axis represents the ratio of array signal intensity for fusion versus wild type, where a positive ratio indicates a increase in fusion copy number. Lone circles represent noise. Strong peaks are clusters of adjacent oligos with altered copy number. Orange, green, or blue arrows and lines indicate deletion, duplication, and triplication, respectively. The X-axis scale is non-linear due to non-uniform oligo density on the arrays, which results in slight smiles in the middle of each chromosome.

Microarray analysis of *ypT21* presented a global view that complemented and exceeded the information provided by inverse PCR. A 2.1 Mb duplication of *IVR* occurred, beginning at an inverted repeat, in agreement with the PCR results. However, starting 4 kb from the *IVR* telomere, there was a 40 kb discontinuity in the duplication, such that this region was present in a wild-type copy number. The 1.2 kb tract of direct subtelomeric repeats present at wild-type *IVR* was excluded from the microarray, as were all highly repetitive sequences, because probes targeting such sequence give poor results. Quite unexpectedly, starting 698 kb from the start of the telomere repeat tract at *XR*, a 301 kb region of the *X* chromosome was triplicated (Figure 4.5). Just to the right of the triplication, a 45 kb duplication and then a 5 kb deletion occurred. Finally, after a 346 kb stretch of *XR* that was present in wild-type copy number, a terminal deletion of 1 kb occurred, in agreement with the terminal deletion determined by inverse PCR. The linear arrangement of the amplifications associated with the *ypT21* breakpoint are presently unclear.

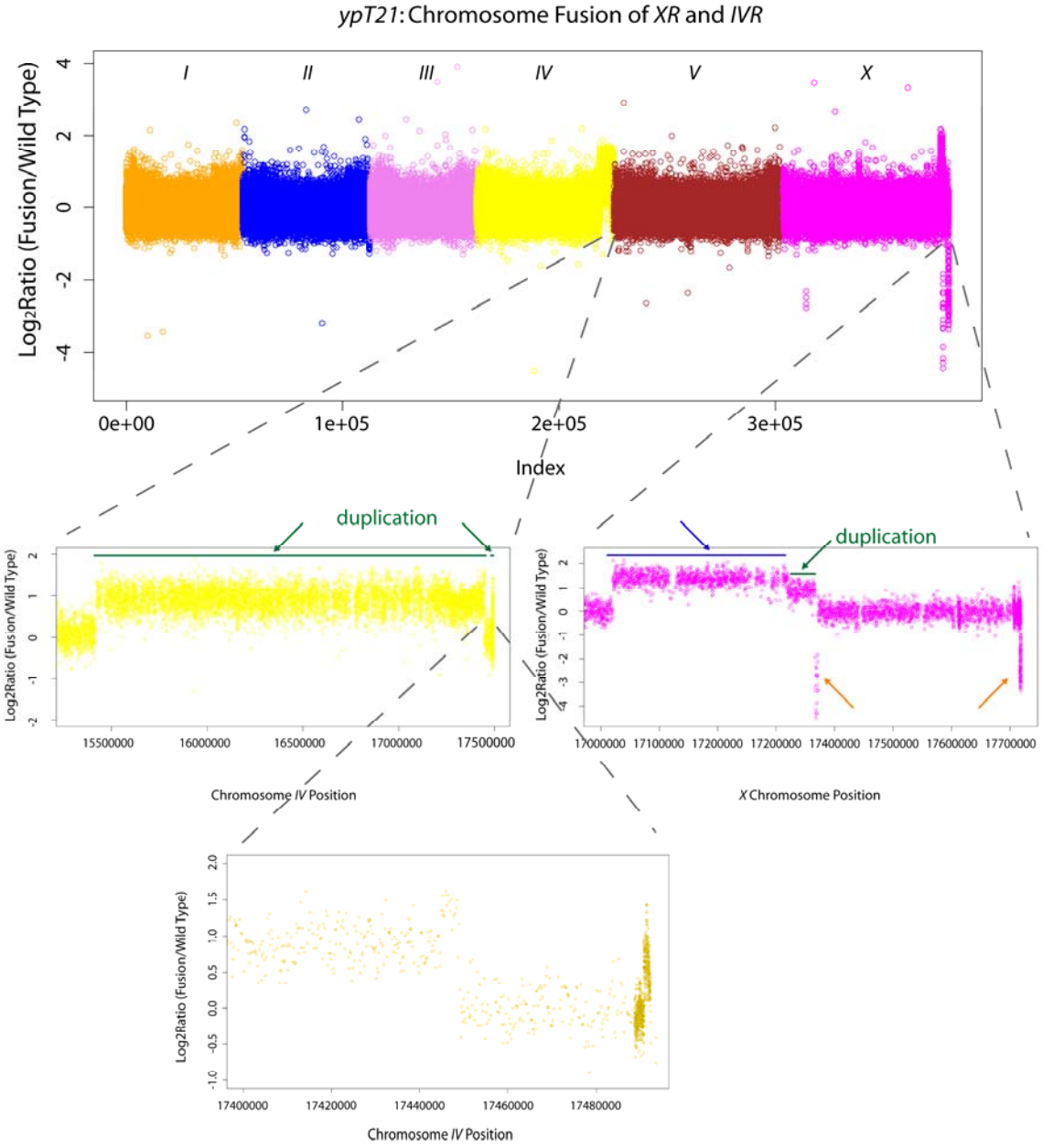

Figure 4.4: Microarray CGH data for *ypT21*. The Y axis represents the ratio of array signal intensity for fusion versus wild type, where a positive ratio indicates a increase in fusion copy number. Lone circles represent noise. Strong peaks are clusters of adjacent oligos with altered copy number. Orange, green, or blue arrows and lines indicate

deletion, duplication, and triplication, respectively. The X axis scale is non-linear due to non-uniform oligo density on the arrays, which results in slight smiles in the middle of each chromosome.

Discussion and Future Directions

We found that end-to-end fusion of the holocentric chromosomes of *C. elegans* resulted in large insertions at some fusion breakpoints. Sequence analysis revealed the identity and orientation of insertions at five fusion breakpoints. For two complex fusion breakpoints, while inverse PCR captured a small part of an insertion and hinted at the size of the insertion, microarray CGH provided a global view of copy number changes in the genome. Only the chromosome ends shown to be fused based on linkage analysis exhibited changes in copy number.

For fusion breakpoints that contained an insertion based on inverse PCR targeting the X chromosome, inverse PCR targeting the fused autosome end failed, despite attempts with different PCR primer pairs and restriction enzymes. It is possible inverted repeats occurred at some autosome fusion breakpoints, perhaps via sister chromatid fusion, which may impede PCR. Alternatively, it could be that, by chance, none of the restriction enzymes used so far were able to make restriction fragments small enough to be amenable to PCR. This seems unlikely because the restriction enzymes used had short target sequences and were likely to be frequent cutters.

In total, 43 fusion events will be analyzed by microarray CGH. Strains that were refractory to PCR and some direct fusions will be tested. Microarray CGH of direct fusions will test the hypothesis that the only aberration associated with direct fusions is direct ligation of two terminally deleted chromosome ends. For the fusions refractory to PCR, microarray CGH will test the hypothesis that insertions occurred. PCR analysis will be used to determine the arrangement of amplifications revealed by microarray analysis. In addition, Southern analysis may be the best approach to test whether inverted repeats

that make a nearly perfect palindrome occurred at fusion breakpoints, given that Capper et al. constructed a model sister chromatid fusion and found that it is refractory to PCR (Capper et al., 2007).

Based on inverse PCR, Southern analysis, and microarray CGH, two fusion breakpoints exhibited a classical combination of rearrangements: inversion, duplication, and deletion. For monocentric chromosomes, heterozygosity for inversion event leads to an inversion loop during meiosis which causes different rearrangements depending on the type of inversion. Meiotic recombination of a pericentric inversion, which involves the centromere, results in chromosomes carrying deletions or duplications. Meiotic recombination of a paracentric inversion, which does not involve the centromere, results in dicentric and acentric chromosomes that each carry deletions or duplications. Although *C. elegans* chromosomes behave as holocentrics during mitosis, they are monocentric during meiosis, when either chromosome end can function as a centromere (Albertson and Thomson, 1993; Zetka and Rose, 1992). Since the centromere is localized to a chromosome end in *C. elegans*, it is likely that inversions are paracentric. Zetka and Rose showed that a *C. elegans* strain carrying an inversion on chromosome *I* produced recombinants carrying deletions and duplications of chromosome *I*, consistent with a paracentric inversion (Zetka and Rose, 1992). Thus, the monocentric behavior of chromosomes during meiosis might predict that although the final product of end-to-end fusion can be stably maintained when chromosome fusions are homozygous, breakage may occur during meiosis when end-to-end chromosome fusions are heterozygous. Thus, the presence of inversion, duplication, and deletion events at fusion breakpoints may be

evidence that breakage has occurred and more than one repair event may mediate a complex fusion.

What predictions can be made for the fusion events that remain to be analyzed by PCR and microarray? One prediction is that fusion breakpoints with terminal deletions at both chromosome fused ends will be direct fusions. However, 6 of 12 such fusion breakpoints have been refractory to PCR with primers facing the fusion breakpoint. We predict that some fusion events will exhibit duplications mediated by recombination or direct ligation, as observed for *ypT27* and *ypT21*. It will be interesting to see the relative frequency of recombination versus direct ligation events and whether the repair event will correlate to the presence of terminal deletions. For example, PCR revealed that chromosome ends with some telomere sequence intact participated in recombination events, while chromosome ends with terminal deletions were involved in direct ligation events. Since only the X chromosome fusion breakpoint was sequenced for each complex fusion and some autosomes were refractory to inverse PCR, microarray analysis may be very useful to provide a basis for additional experiments. It could be that for the fusion strains with insertions of the autosome, a sister chromatid fusion is present at the autosome breakpoint. The orientation of the insertion is consistent with this possibility. However, in contrast to this somewhat simple possibility, microarray analysis of *ypT21* revealed that both chromosome ends involved in the fusion event can experience amplification. Finally, microarray analysis may reveal new rearrangements, such as amplification of genomic DNA not implicated by linkage analysis. Even though such an event was not predicted by the pilot microarray results, a larger sample size may contain a broader spectrum of complex rearrangements.

In addition to the possibility that chromosome rearrangements subsequent to telomere dysfunction may contribute to oncogenesis, rearrangement of subtelomeric DNA commonly occurs during genome evolution (Linardopoulou et al., 2005; Murnane and Sabatier, 2004). Chromosome size varies from one person to another by as much as 10-45% and most of the variability is due to alteration of pericentromeric and subtelomeric sequences (Knight, 2002; Mefford et al., 1997; Trask et al., 1989; Wilkie et al., 1991). In the last 5 million years, half of the sequence at human subtelomeres (1.13 Mb) arose from NHEJ events followed by interchromosomal recombination events, such that blocks of DNA 13 to 500 kb are present at multiple subtelomeres (Ambrosini et al., 2007; Linardopoulou et al., 2005). Thus, subtelomeres are a patchwork of duplications that appear on many chromosome ends (Linardopoulou et al., 2005). At the boundaries of nearly all these duplications are internal telomeric tracts, suggesting they may be remnants of telomere-telomere fusion events or may have played a role in creating the complex organization at human subtelomeres (Ambrosini et al., 2007). In support of the first prospect, in normal proliferating or senescent cultured human cells, sudden stochastic deletion events can create critically shortened telomeres that fuse at a frequency of 4×10^{-6}, even when most telomeres are of normal length (Capper et al., 2007). Fusion of sporadic uncapped telomeres occurs in both telomerase-deficient and telomerase-expressing cell lines (Capper et al., 2007). In agreement with a possible mechanistic role for internal telomeric tracts, we showed that two cases of recombination occurred between an uncapped *XR* telomere and the internal telomeric tract that was closest to the *XR* telomere (Figure 4.5). This suggests that the site of recombination was not random and that the internal telomeric tracts may be nucleating the recombination

events. For the third fusion breakpoint involving telomere recombination, an uncapped *XL* telomere recombined with the internal telomere tract that was fifth closest to *IVL*. This event originated in a *mrt-2* strain, which is partially defective for homologous recombination. Perhaps the defect in homologous recombination explains why an autosome was targeted or why internal telomeric repeat tract closest to the *IVL* telomere was not used. Thus, on a large time scale, recombination events involving uncapped telomeres may drive evolution of human subtelomeres. This process may be recapitulated on a much shorter time scale in turmorigenesis and in *C. elegans* telomerase mutants.

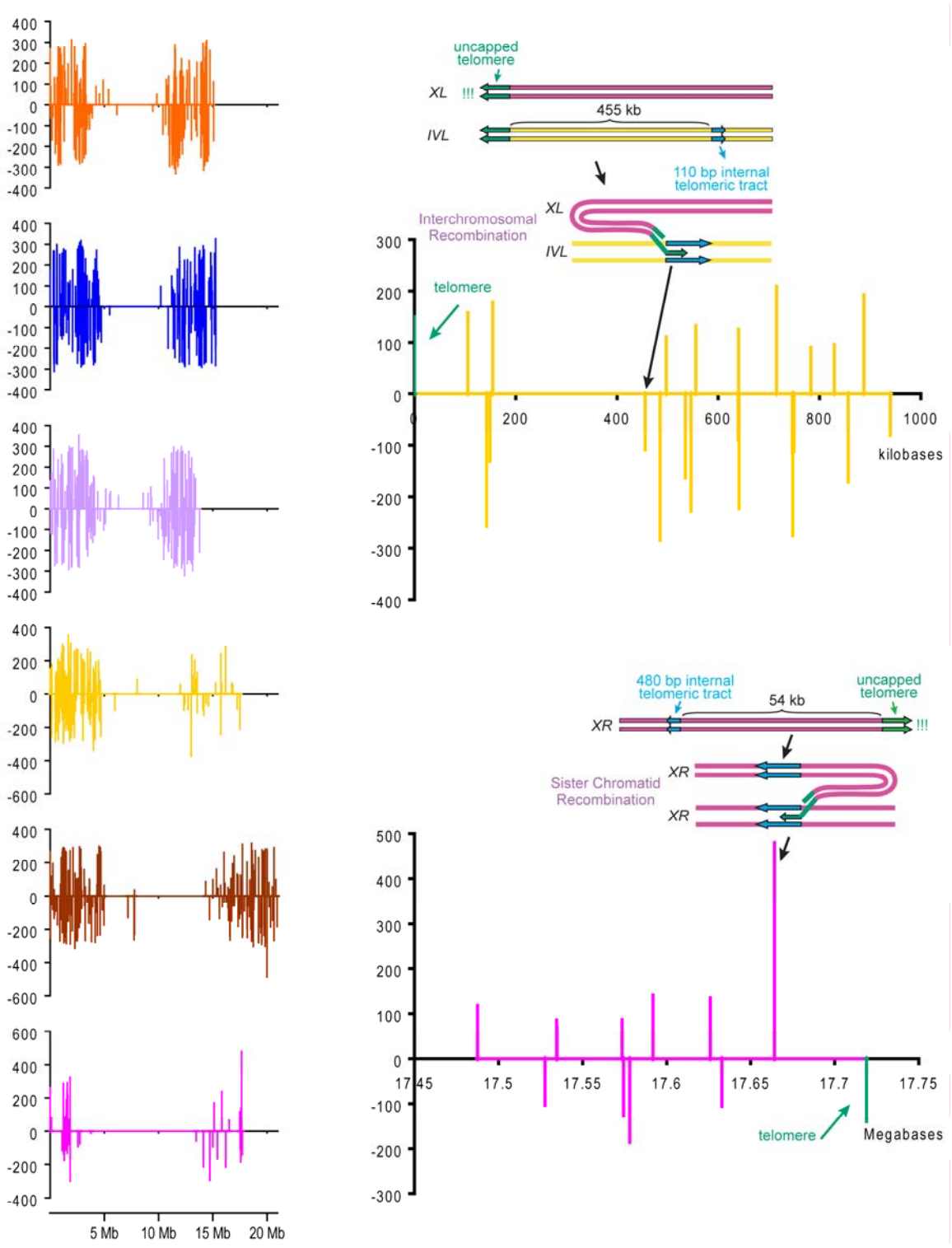

Figure 4.5: Distribution of internal telomeric repeat tracts. The plots show the positions of 1,381 internal telomeric repeat tracts on the six chromosomes of *C. elegans*.

The X-axis represents chromosome position. The Y-axis represents the length and orientation of the internal telomeric repeats. Vertical lines extending above or below zero correspond to tracts in a forward or reverse orientation along the chromosome, respectively. The vertical lines at the extreme left or right of each plot correspond to the telomeres, and the colored horizontal line demarcates the extend of the chromosome. The internal telomeric repeat tracts (blue block arrow) involved in recombination events with uncapped telomere (green block arrow) are shown on the right, along with all of the tracts that occur in the last 1 Mb of *IVL* or *XR*.

While cytogenetic measurements can show chromosomal alterations at a gross level, simultaneous sequence and physical analysis of a rearrangement triggered by telomere uncapping is difficult in most systems. It is intriguing that we have observed large telomeric duplication and triplication events that may be analogous to events that shape our own rapidly evolving subtelomeric DNA, which is a complex and highly heterogeneous portion of the human genome that may contribute substantially to the diversity of phenotypes that occur in the human race. Thus, the studies described here may eventually provide mechanistic insights into an important phenomenon relevant to genome evolution: the molecular basis of chromosomal rearrangements triggered by telomere uncapping.

CHAPTER 5

CONCLUDING REMARKS

Contribution to telomere field

The primary goal of this study was to examine repair events at uncapped telomeres in *C. elegans* to provide a model for the genesis of end-to-end chromosome fusions. *C. elegans* is uniquely suitable to address this issue, allowing a broader spectrum of fusion events to be studied at the molecular level than has been possible previously in other organisms (Capper et al., 2007; Cheung et al., 2006; Hackett et al., 2001; Heacock et al., 2004; Hemann et al., 2001; Mieczkowski et al., 2003). Our study was not fully dependent on the generation of a PCR product or biased by using PCR primers targeted very close to the telomere. Another advantage was that we could perform Southern blots or microarray analysis to provide physical evidence to verify the PCR data. This study took advantage of a variety of approaches available in *C. elegans* to elucidate the molecular structure of end-to-end chromosome fusions.

This work will change how the field of telomeres looks at the fate of dysfunctional telomeres. Previous studies suggest that direct ligation is the predominant repair event at uncapped telomeres. Based on molecular and physical analysis of genetically isolated end-to-end chromosome fusions, we conclude that while direct ligation occurred at some fusion breakpoints, complex events involving amplification of large segments of genomic

DNA drive end-to-end fusion. The results of inverse PCR and the pilot microarray experiment suggest that inversions may occur at fusion breakpoints. The model that inversion may promote duplications and deletions will provide a starting point to investigate the linear order of segmental amplifications and deletions. A more complete model of genesis of end-to-end fusions awaits additional microarray CGH, accompanied by PCR and Southern analysis, which should reveal more about the complex events.

The results described here will help to develop *C. elegans* as a system to study telomere dysfunction, which occurs in aged and cancer cells in humans. *C. elegans* provides a genetically tractable model to find genes required for telomere function and allows the consequences of telomere dysfunction to be examined at the molecular level. Rearrangement of chromosomes contributes to oncogenesis (reviewed in Gebhart, 2005) and other types of human disease (reviewed in Shaw and Lupski, 2004). Subtelomeres are hot spots of recombination between chromosomes (Linardopoulou et al., 2005), and the rearrangements described here may contribute to models of genome evolution, if occasional uncapping and fusion of telomeres is a natural occurrence.

Contribution to *C. elegans* field

We also investigated whether a core component of NHEJ contributes to telomere lengths homeostasis: the Ku heterodimer, an NHEJ component whose functions in telomere biology are well-studied, if somewhat plastic and controversial (reviewed in Fisher and Zakian, 2005; reviewed in Slijepcevic, 2006). This work contributes to the development of *C. elegans* as a model for telomeres by establishing that Ku has no

synthetic effects with telomerase. In this respect, the telomere biology of *C. elegans* is like that of mice.

This work provides a fantastic resource to the *C. elegans* community by providing ~50 characterized translocations and deletions that could be used for many applications. Already we have two collaborators using the strains to understand how dosage compensation complexes behave at the breakpoint of an *X*-autosome translocation: does the complex spread from the *X* chromosome to the autosome, and if so how far does it spread? Precisely mapped breakpoints offer a wonderful starting point to address this question. Another collaborator will use *ypT41*, which contains a direct fusion of *XR* and *IIL*, for complementation analysis to map an apoptosis mutation. The mutation is near *sqt-2*, which is deleted in *ypT41*, but low rates of recombination in the area have hampered mapping. Thus, the fusion strains can be used to study a variety of areas unrelated to telomere uncapping.

References

Ahmed, S. and Hodgkin, J. (2000) MRT-2 checkpoint protein is required for germline immortality and telomere replication in C. elegans. *Nature*, 403, 159-164.

Albertson, D.G. and Thomson, J.N. (1993) Segregation of holocentric chromosomes at meiosis in the nematode, Caenorhabditis elegans. *Chromosome Res*, 1, 15-26.

Allsopp, R.C., Cheshier, S. and Weissman, I.L. (2001) Telomere shortening accompanies increased cell cycle activity during serial transplantation of hematopoietic stem cells. *J Exp Med*, 193, 917-924.

Ambrosini, A., Paul, S., Hu, S. and Riethman, H. (2007) Human subtelomeric duplicon structure and organization. *Genome Biol*, 8, R151.

Bae, N.S. and Baumann, P. (2007) A RAP1/TRF2 complex inhibits nonhomologous end-joining at human telomeric DNA ends. *Mol Cell*, 26, 323-334.

Bailey, S.M., Brenneman, M.A., Halbrook, J., Nickoloff, J.A., Ullrich, R.L. and Goodwin, E.H. (2004) The kinase activity of DNA-PK is required to protect mammalian telomeres. *DNA Repair (Amst)*, 3, 225-233.

Bailey, S.M., Meyne, J., Chen, D.J., Kurimasa, A., Li, G.C., Lehnert, B.E. and Goodwin, E.H. (1999) DNA double-strand break repair proteins are required to cap the ends of mammalian chromosomes. *Proc Natl Acad Sci U S A*, 96, 14899-14904.

Bailey, S.M. and Murnane, J.P. (2006) Telomeres, chromosome instability and cancer. *Nucleic Acids Res*, 34, 2408-2417.

Barnes, D.E., Stamp, G., Rosewell, I., Denzel, A. and Lindahl, T. (1998) Targeted disruption of the gene encoding DNA ligase IV leads to lethality in embryonic mice. *Curr Biol*, 8, 1395-1398.

Baumann, P. and Cech, T.R. (2000) Protection of telomeres by the Ku protein in fission yeast. *Mol Biol Cell*, 11, 3265-3275.

Baumann, P. and Cech, T.R. (2001) Pot1, the putative telomere end-binding protein in fission yeast and humans. *Science*, 292, 1171-1175.

Bechter, O.E., Zou, Y., Shay, J.W. and Wright, W.E. (2003) Homologous recombination in human telomerase-positive and ALT cells occurs with the same frequency. *EMBO Rep*, 4, 1138-1143.

Bentley, J., Diggle, C.P., Harnden, P., Knowles, M.A. and Kiltie, A.E. (2004) DNA double strand break repair in human bladder cancer is error prone and involves microhomology-associated end-joining. *Nucleic Acids Res*, 32, 5249-5259.

Bertuch, A.A. and Lundblad, V. (2003) The Ku heterodimer performs separable activities at double-strand breaks and chromosome termini. *Mol Cell Biol*, 23, 8202-8215.

Blackburn, E.H. and Gall, J.G. (1978) A tandemly repeated sequence at the termini of the extrachromosomal ribosomal RNA genes in Tetrahymena. *J Mol Biol*, 120, 33-53.

Boerckel, J., Walker, D. and Ahmed, S. (2007) The C. elegans Rad17 homolog HPR-17 is required for telomere replication. *Genetics*, genetics.106.070201.

Boulton, S.J. and Jackson, S.P. (1996a) Identification of a Saccharomyces cerevisiae Ku80 homologue: roles in DNA double strand break rejoining and in telomeric maintenance. *Nucleic Acids Res*, 24, 4639-4648.

Boulton, S.J. and Jackson, S.P. (1996b) Saccharomyces cerevisiae Ku70 potentiates illegitimate DNA double-strand break repair and serves as a barrier to error-prone DNA repair pathways. *Embo J*, 15, 5093-5103.

Broccoli, D., Young, J.W. and de Lange, T. (1995) Telomerase activity in normal and malignant hematopoietic cells. *Proc Natl Acad Sci U S A*, 92, 9082-9086.

Brown, W.R., Dobson, M.J. and MacKinnon, P. (1990) Telomere cloning and mammalian chromosome analysis. *J Cell Sci*, 95 (Pt 4), 521-526.

Burr, B., Burr, F.A., Matz, E.C. and Romero-Severson, J. (1992) Pinning down loose ends: mapping telomeres and factors affecting their length. *Plant Cell*, 4, 953-960.

Capper, R., Britt-Compton, B., Tankimanova, M., Rowson, J., Letsolo, B., Man, S., Haughton, M. and Baird, D.M. (2007) The nature of telomere fusion and a definition of the critical telomere length in human cells. *Genes Dev*, 21, 2495-2508.

Carter, S.D., Iyer, S., Xu, J., McEachern, M.J. and Astrom, S.U. (2007) The Role Of NHEJ-Components In Telomere Metabolism In Kluyveromyces lactis. *Genetics*.

Cech, T.R. (2004) Beginning to understand the end of the chromosome. *Cell*, 116, 273-279.

Cheung, I., Schertzer, M., Rose, A. and Lansdorp, P.M. (2006) High incidence of rapid telomere loss in telomerase-deficient Caenorhabditis elegans. *Nucleic Acids Res*, 34, 96-103.

Clejan, I., Boerckel, J. and Ahmed, S. (2006) Developmental modulation of nonhomologous end joining in Caenorhabditis elegans. *Genetics*, 173, 1301-1317.

d'Adda di Fagagna, F., Hande, M.P., Tong, W.M., Roth, D., Lansdorp, P.M., Wang, Z.Q. and Jackson, S.P. (2001) Effects of DNA nonhomologous end-joining factors on telomere length and chromosomal stability in mammalian cells. *Curr Biol*, 11, 1192-1196.

d'Adda di Fagagna, F., Reaper, P.M., Clay-Farrace, L., Fiegler, H., Carr, P., Von Zglinicki, T., Saretzki, G., Carter, N.P. and Jackson, S.P. (2003) A DNA damage checkpoint response in telomere-initiated senescence. *Nature*, 426, 194-198.

de Lange, T. (2004) T-loops and the origin of telomeres. *Nat Rev Mol Cell Biol*, 5, 323-329.

de Lange, T. (2005) Shelterin: the protein complex that shapes and safeguards human telomeres. *Genes Dev*, 19, 2100-2110.

Decottignies, A. (2007) Microhomology-mediated end joining in fission yeast is repressed by pku70 and relies on genes involved in homologous recombination. *Genetics*, 176, 1403-1415.

Diede, S.J. and Gottschling, D.E. (1999) Telomerase-mediated telomere addition in vivo requires DNA primase and DNA polymerases alpha and delta. *Cell*, 99, 723-733.

Difilippantonio, M.J., Zhu, J., Chen, H.T., Meffre, E., Nussenzweig, M.C., Max, E.E., Ried, T. and Nussenzweig, A. (2000) DNA repair protein Ku80 suppresses chromosomal aberrations and malignant transformation. *Nature*, 404, 510-514.

Dunham, M.A., Neumann, A.A., Fasching, C.L. and Reddel, R.R. (2000) Telomere maintenance by recombination in human cells. *Nat Genet*, 26, 447-450.

Espejel, S. and Blasco, M.A. (2002) Identification of telomere-dependent "senescence-like" arrest in mouse embryonic fibroblasts. *Exp Cell Res*, 276, 242-248.

Espejel, S., Franco, S., Rodriguez-Perales, S., Bouffler, S.D., Cigudosa, J.C. and Blasco, M.A. (2002a) Mammalian Ku86 mediates chromosomal fusions and apoptosis caused by critically short telomeres. *Embo J*, 21, 2207-2219.

Espejel, S., Franco, S., Sgura, A., Gae, D., Bailey, S.M., Taccioli, G.E. and Blasco, M.A. (2002b) Functional interaction between DNA-PKcs and telomerase in telomere length maintenance. *Embo J*, 21, 6275-6287.

Feldmann, E., Schmiemann, V., Goedecke, W., Reichenberger, S. and Pfeiffer, P. (2000) DNA double-strand break repair in cell-free extracts from Ku80-deficient cells: implications for Ku serving as an alignment factor in non-homologous DNA end joining. *Nucleic Acids Res*, 28, 2585-2596.

Ferreira, M.G. and Cooper, J.P. (2001) The fission yeast Taz1 protein protects chromosomes from Ku-dependent end-to-end fusions. *Mol Cell*, 7, 55-63.

Fisher, T.S. and Zakian, V.A. (2005) Ku: a multifunctional protein involved in telomere maintenance. *DNA Repair (Amst)*, 4, 1215-1226.

Foreman, K.E. and Tang, J. (2003) Molecular mechanisms of replicative senescence in endothelial cells. *Exp Gerontol*, 38, 1251-1257.

Gallego, M.E., Jalut, N. and White, C.I. (2003) Telomerase dependence of telomere lengthening in Ku80 mutant Arabidopsis. *Plant Cell*, 15, 782-789.

Gebhart, E. (2005) Genomic imbalances in human leukemia and lymphoma detected by comparative genomic hybridization (Review). *Int J Oncol*, 27, 593-606.

Gilley, D., Tanaka, H., Hande, M.P., Kurimasa, A., Li, G.C., Oshimura, M. and Chen, D.J. (2001) DNA-PKcs is critical for telomere capping. *Proc Natl Acad Sci U S A*, 98, 15084-15088.

Gire, V., Roux, P., Wynford-Thomas, D., Brondello, J.M. and Dulic, V. (2004) DNA damage checkpoint kinase Chk2 triggers replicative senescence. *Embo J*, 23, 2554-2563.

Goytisolo, F.A., Samper, E., Edmonson, S., Taccioli, G.E. and Blasco, M.A. (2001) The absence of the dna-dependent protein kinase catalytic subunit in mice results in anaphase bridges and in increased telomeric fusions with normal telomere length and G-strand overhang. *Mol Cell Biol*, 21, 3642-3651.

Gravel, S., Larrivee, M., Labrecque, P. and Wellinger, R.J. (1998) Yeast Ku as a regulator of chromosomal DNA end structure. *Science*, 280, 741-744.

Greider, C.W. and Blackburn, E.H. (1985) Identification of a specific telomere terminal transferase activity in Tetrahymena extracts. *Cell*, 43, 405-413.

Greider, C.W. and Blackburn, E.H. (1987) The telomere terminal transferase of Tetrahymena is a ribonucleoprotein enzyme with two kinds of primer specificity. *Cell*, 51, 887-898.

Griffith, J.D., Comeau, L., Rosenfield, S., Stansel, R.M., Bianchi, A., Moss, H. and de Lange, T. (1999) Mammalian telomeres end in a large duplex loop. *Cell*, 97, 503-514.

Guirouilh-Barbat, J., Huck, S., Bertrand, P., Pirzio, L., Desmaze, C., Sabatier, L. and Lopez, B.S. (2004) Impact of the KU80 pathway on NHEJ-induced genome rearrangements in mammalian cells. *Mol Cell*, 14, 611-623.

Hackett, J.A., Feldser, D.M. and Greider, C.W. (2001) Telomere dysfunction increases mutation rate and genomic instability. *Cell*, 106, 275-286.

Harle-Bachor, C. and Boukamp, P. (1996) Telomerase activity in the regenerative basal layer of the epidermis inhuman skin and in immortal and carcinoma-derived skin keratinocytes. *Proc Natl Acad Sci U S A*, 93, 6476-6481.

Harley, C.B., Futcher, A.B. and Greider, C.W. (1990) Telomeres shorten during ageing of human fibroblasts. *Nature*, 345, 458-460.

Hastie, N.D., Dempster, M., Dunlop, M.G., Thompson, A.M., Green, D.K. and Allshire, R.C. (1990) Telomere reduction in human colorectal carcinoma and with ageing. *Nature*, 346, 866-868.

Hayflick, L. and Moorhead, P.S. (1961) The serial cultivation of human diploid cell strains. *Exp Cell Res*, 25, 585-621.

Heacock, M., Spangler, E., Riha, K., Puizina, J. and Shippen, D.E. (2004) Molecular analysis of telomere fusions in Arabidopsis: multiple pathways for chromosome end-joining. *Embo J*, 23, 2304-2313.

Hemann, M.T., Strong, M.A., Hao, L.Y. and Greider, C.W. (2001) The shortest telomere, not average telomere length, is critical for cell viability and chromosome stability. *Cell*, 107, 67-77.

Henson, J.D., Neumann, A.A., Yeager, T.R. and Reddel, R.R. (2002) Alternative lengthening of telomeres in mammalian cells. *Oncogene*, 21, 598-610.

Herman, R.K. and Kari, C.K. (1989) Recombination Between Small X-Chromosome Duplications And The X-Chromosome In Caenorhabditis-Elegans. *Genetics*, 121, 723-737.

Herman, R.K., Kari, C.K. and Hartman, P.S. (1982) Dominant X-chromosome nondisjunction mutants of Caenorhabditis elegans. *Genetics*, 102, 379-400.

Hiyama, K., Hirai, Y., Kyoizumi, S., Akiyama, M., Hiyama, E., Piatyszek, M.A., Shay, J.W., Ishioka, S. and Yamakido, M. (1995) Activation of telomerase in human lymphocytes and hematopoietic progenitor cells. *J Immunol*, 155, 3711-3715.

Hodgkin, J., Horvitz, H.R. and Brenner, S. (1979) Nondisjunction Mutants of the Nematode CAENORHABDITIS ELEGANS. *Genetics*, 91, 67-94.

Hofmann, E.R., Milstein, S., Boulton, S.J., Ye, M., Hofmann, J.J., Stergiou, L., Gartner, A., Vidal, M. and Hengartner, M.O. (2002) Caenorhabditis elegans HUS-1 is a DNA damage checkpoint protein required for genome stability and EGL-1-mediated apoptosis. *Curr Biol*, 12, 1908-1918.

Hsu, H.L., Gilley, D., Galande, S.A., Hande, M.P., Allen, B., Kim, S.H., Li, G.C., Campisi, J., Kohwi-Shigematsu, T. and Chen, D.J. (2000) Ku acts in a unique way at the mammalian telomere to prevent end joining. *Genes Dev*, 14, 2807-2812.

http://www.wormbase.org.

Hug, N. and Lingner, J. (2006) Telomere length homeostasis. *Chromosoma*, 115, 413-425.

Jaco, I., Munoz, P. and Blasco, M.A. (2004) Role of human Ku86 in telomere length maintenance and telomere capping. *Cancer Res*, 64, 7271-7278.

Jarrard, D.F., Sarkar, S., Shi, Y., Yeager, T.R., Magrane, G., Kinoshita, H., Nassif, N., Meisner, L., Newton, M.A., Waldman, F.M. and Reznikoff, C.A. (1999) p16/pRb pathway alterations are required for bypassing senescence in human prostate epithelial cells. *Cancer Res*, 59, 2957-2964.

Kabotyanski, E.B., Gomelsky, L., Han, J.O., Stamato, T.D. and Roth, D.B. (1998) Double-strand break repair in Ku86- and XRCC4-deficient cells. *Nucleic Acids Res*, 26, 5333-5342.

Kibe, T., Tomita, K., Matsuura, A., Izawa, D., Kodaira, T., Ushimaru, T., Uritani, M. and Ueno, M. (2003) Fission yeast Rhp51 is required for the maintenance of telomere structure in the absence of the Ku heterodimer. *Nucleic Acids Res*, 31, 5054-5063.

Kipling, D. and Cooke, H.J. (1990) Hypervariable ultra-long telomeres in mice. *Nature*, 347, 400-402.

Kirk, K.E., Harmon, B.P., Reichardt, I.K., Sedat, J.W. and Blackburn, E.H. (1997) Block in anaphase chromosome separation caused by a telomerase template mutation. *Science*, 275, 1478-1481.

Kiyono, T., Foster, S.A., Koop, J.I., McDougall, J.K., Galloway, D.A. and Klingelhutz, A.J. (1998) Both Rb/p16INK4a inactivation and telomerase activity are required to immortalize human epithelial cells. *Nature*, 396, 84-88.

Knight, J. (2002) All genomes great and small. *Nature*, 417, 374-376.

Kornberg, A. (1974) *DNA Synthesis*.

Kusch, M. and Edgar, R.S. (1986) Genetic studies of unusual loci that affect body shape of the nematode Caenorhabditis elegans and may code for cuticle structural proteins. *Genetics*, 113, 621-639.

Lansdorp, P.M. (2005) Major cutbacks at chromosome ends. *Trends Biochem Sci*, 30, 388-395.

Levis, R.W., Ganesan, R., Houtchens, K., Tolar, L.A. and Sheen, F.M. (1993) Transposons in place of telomeric repeats at a Drosophila telomere. *Cell*, 75, 1083-1093.

Li, G., Nelsen, C. and Hendrickson, E.A. (2002) Ku86 is essential in human somatic cells. *Proc Natl Acad Sci U S A*, 99, 832-837.

Lieber, M.R. (1999) The biochemistry and biological significance of nonhomologous DNA end joining: an essential repair process in multicellular eukaryotes. *Genes Cells*, 4, 77-85.

Linardopoulou, E.V., Williams, E.M., Fan, Y., Friedman, C., Young, J.M. and Trask, B.J. (2005) Human subtelomeres are hot spots of interchromosomal recombination and segmental duplication. *Nature*, 437, 94-100.

Lingner, J., Hughes, T.R., Shevchenko, A., Mann, M., Lundblad, V. and Cech, T.R. (1997) Reverse transcriptase motifs in the catalytic subunit of telomerase. *Science*, 276, 561-567.

Liu, K., Schoonmaker, M.M., Levine, B.L., June, C.H., Hodes, R.J. and Weng, N.P. (1999) Constitutive and regulated expression of telomerase reverse transcriptase (hTERT) in human lymphocytes. *Proc Natl Acad Sci U S A*, 96, 5147-5152.

Loayza, D. and De Lange, T. (2003) POT1 as a terminal transducer of TRF1 telomere length control. *Nature*, 423, 1013-1018.

Lobachev, K.S., Shor, B.M., Tran, H.T., Taylor, W., Keen, J.D., Resnick, M.A. and Gordenin, D.A. (1998) Factors affecting inverted repeat stimulation of recombination and deletion in Saccharomyces cerevisiae. *Genetics*, 148, 1507-1524.

Lobachev, K.S., Stenger, J.E., Kozyreva, O.G., Jurka, J., Gordenin, D.A. and Resnick, M.A. (2000) Inverted Alu repeats unstable in yeast are excluded from the human genome. *Embo J*, 19, 3822-3830.

Lombard, D.B. and Guarente, L. (2000) Nijmegen breakage syndrome disease protein and MRE11 at PML nuclear bodies and meiotic telomeres. *Cancer Res*, 60, 2331-2334.

Lydall, D. (2003) Hiding at the ends of yeast chromosomes: telomeres, nucleases and checkpoint pathways. *J Cell Sci*, 116, 4057-4065.

Ma, J.L., Kim, E.M., Haber, J.E. and Lee, S.E. (2003) Yeast Mre11 and Rad1 proteins define a Ku-independent mechanism to repair double-strand breaks lacking overlapping end sequences. *Mol Cell Biol*, 23, 8820-8828.

Manolis, K.G., Nimmo, E.R., Hartsuiker, E., Carr, A.M., Jeggo, P.A. and Allshire, R.C. (2001) Novel functional requirements for non-homologous DNA end joining in Schizosaccharomyces pombe. *Embo J*, 20, 210-221.

Maringele, L. and Lydall, D. (2004) EXO1 plays a role in generating type I and type II survivors in budding yeast. *Genetics*, 166, 1641-1649.

Maser, R.S., Wong, K.K., Sahin, E., Xia, H., Naylor, M., Hedberg, H.M., Artandi, S.E. and Depinho, R.A. (2007) DNA-PKcs is not required for dysfunctional telomere fusion and checkpoint response in the telomerase deficient mouse. ***Mol Cell Biol.***

Masutomi, K., Yu, E.Y., Khurts, S., Ben-Porath, I., Currier, J.L., Metz, G.B., Brooks, M.W., Kaneko, S., Murakami, S., DeCaprio, J.A., Weinberg, R.A., Stewart, S.A. and Hahn, W.C. (2003) Telomerase maintains telomere structure in normal human cells. ***Cell,*** **114, 241-253.**

Maydan, J.S., Flibotte, S., Edgley, M.L., Lau, J., Selzer, R.R., Richmond, T.A., Pofahl, N.J., Thomas, J.H. and Moerman, D.G. (2007) Efficient high-resolution deletion discovery in Caenorhabditis elegans by array comparative genomic hybridization. ***Genome Res,*** **17, 337-347.**

McClintock, B. (1941) THE STABILITY OF BROKEN ENDS OF CHROMOSOMES IN ZEA MAYS. ***Genetics,*** **26, 234-282.**

McEachern, M.J. and Blackburn, E.H. (1995) Runaway telomere elongation caused by telomerase RNA gene mutations. ***Nature,*** **376, 403-409.**

Mefford, H., van den Engh, G., Friedman, C. and Trask, B.J. (1997) Analysis of the variation in chromosome size among diverse human populations by bivariate flow karyotyping. ***Hum Genet,*** **100, 138-144.**

Meier, B., Clejan, I., Liu, Y., Lowden, M., Gartner, A., Hodgkin, J. and Ahmed, S. (2006) trt-1 is the Caenorhabditis elegans catalytic subunit of telomerase. ***PLoS Genet,*** **2, e18.**

Mieczkowski, P.A., Mieczkowska, J.O., Dominska, M. and Petes, T.D. (2003) Genetic regulation of telomere-telomere fusions in the yeast Saccharomyces cerevisae. ***Proc Natl Acad Sci U S A,*** **100, 10854-10859.**

Miller, K.M., Ferreira, M.G. and Cooper, J.P. (2005) Taz1, Rap1 and Rif1 act both interdependently and independently to maintain telomeres. ***Embo J,*** **24, 3128-3135.**

Moore, J.K. and Haber, J.E. (1996) Cell cycle and genetic requirements of two pathways of nonhomologous end-joining repair of double-strand breaks in Saccharomyces cerevisiae. ***Mol Cell Biol,*** **16, 2164-2173.**

Moyzis, R.K., Buckingham, J.M., Cram, L.S., Dani, M., Deaven, L.L., Jones, M.D., Meyne, J., Ratliff, R.L. and Wu, J.R. (1988) A highly conserved repetitive DNA sequence, (TTAGGG)n, present at the telomeres of human chromosomes. *Proc Natl Acad Sci U S A*, 85, 6622-6626.

Müller, H. (1938) The remaking of chromosomes. *Collecting Net*, 13, 181–195.

Murnane, J.P. and Sabatier, L. (2004) Chromosome rearrangements resulting from telomere dysfunction and their role in cancer. *Bioessays*, 26, 1164-1174.

Murnane, J.P., Sabatier, L., Marder, B.A. and Morgan, W.F. (1994) Telomere dynamics in an immortal human cell line. *Embo J*, 13, 4953-4962.

Myung, K., Ghosh, G., Fattah, F.J., Li, G., Kim, H., Dutia, A., Pak, E., Smith, S. and Hendrickson, E.A. (2004) Regulation of telomere length and suppression of genomic instability in human somatic cells by Ku86. *Mol Cell Biol*, 24, 5050-5059.

Nakamura, T.M., Morin, G.B., Chapman, K.B., Weinrich, S.L., Andrews, W.H., Lingner, J., Harley, C.B. and Cech, T.R. (1997) Telomerase catalytic subunit homologs from fission yeast and human. *Science*, 277, 955-959.

Nugent, C.I., Bosco, G., Ross, L.O., Evans, S.K., Salinger, A.P., Moore, J.K., Haber, J.E. and Lundblad, V. (1998) Telomere maintenance is dependent on activities required for end repair of double-strand breaks. *Curr Biol*, 8, 657-660.

Ohki, R., Tsurimoto, T. and Ishikawa, F. (2001) In vitro reconstitution of the end replication problem. *Mol Cell Biol*, 21, 5753-5766.

Olovnikov, A.M. (1973) A theory of marginotomy. The incomplete copying of template margin in enzymic synthesis of polynucleotides and biological significance of the phenomenon. *J Theor Biol*, 41, 181-190.

Pardo, B. and Marcand, S. (2005) Rap1 prevents telomere fusions by nonhomologous end joining. *Embo J*, 24, 3117-3127.

Perou, C.M., Sorlie, T., Eisen, M.B., van de Rijn, M., Jeffrey, S.S., Rees, C.A., Pollack, J.R., Ross, D.T., Johnsen, H., Akslen, L.A., Fluge, O.,

Pergamenschikov, A., Williams, C., Zhu, S.X., Lonning, P.E., Borresen-Dale, A.L., Brown, P.O. and Botstein, D. (2000) Molecular portraits of human breast tumours. *Nature*, 406, 747-752.

Pollack, J.R., Sorlie, T., Perou, C.M., Rees, C.A., Jeffrey, S.S., Lonning, P.E., Tibshirani, R., Botstein, D., Borresen-Dale, A.L. and Brown, P.O. (2002) Microarray analysis reveals a major direct role of DNA copy number alteration in the transcriptional program of human breast tumors. *Proc Natl Acad Sci U S A*, 99, 12963-12968.

Polotnianka, R.M., Li, J. and Lustig, A.J. (1998) The yeast Ku heterodimer is essential for protection of the telomere against nucleolytic and recombinational activities. *Curr Biol*, 8, 831-834.

Porter, S.E., Greenwell, P.W., Ritchie, K.B. and Petes, T.D. (1996) The DNA-binding protein Hdf1p (a putative Ku homologue) is required for maintaining normal telomere length in Saccharomyces cerevisiae. *Nucleic Acids Res*, 24, 582-585.

Prescott, J. and Blackburn, E.H. (1997) Telomerase RNA mutations in Saccharomyces cerevisiae alter telomerase action and reveal nonprocessivity in vivo and in vitro. *Genes Dev.*, 11, 528-540.

Reaper, P.M., di Fagagna, F. and Jackson, S.P. (2004) Activation of the DNA damage response by telomere attrition: a passage to cellular senescence. *Cell Cycle*, 3, 543-546.

Riha, K., Heacock, M.L. and Shippen, D.E. (2006) The role of the nonhomologous end-joining DNA double-strand break repair pathway in telomere biology. *Annu Rev Genet*, 40, 237-277.

Riha, K. and Shippen, D.E. (2003) Ku is required for telomeric C-rich strand maintenance but not for end-to-end chromosome fusions in Arabidopsis. *Proc Natl Acad Sci U S A*, 100, 611-615.

Riha, K., Watson, J.M., Parkey, J. and Shippen, D.E. (2002) Telomere length deregulation and enhanced sensitivity to genotoxic stress in Arabidopsis mutants deficient in Ku70. *Embo J*, 21, 2819-2826.

Robert, V. and Bessereau, J.L. (2007) Targeted engineering of the Caenorhabditis elegans genome following Mos1-triggered chromosomal breaks. *Embo J*, 26, 170-183.

Samper, E., Goytisolo, F.A., Slijepcevic, P., van Buul, P.P. and Blasco, M.A. (2000) Mammalian Ku86 protein prevents telomeric fusions independently of the length of TTAGGG repeats and the G-strand overhang. *EMBO Rep*, 1, 244-252.

Sanger, F., Nicklen, S. and Coulson, A.R. (1977) DNA sequencing with chain-terminating inhibitors. *Proc Natl Acad Sci U S A*, 74, 5463-5467.

Sfeir, A.J., Chai, W., Shay, J.W. and Wright, W.E. (2005) Telomere-end processing the terminal nucleotides of human chromosomes. *Mol Cell*, 18, 131-138.

Shakirov, E.V., Surovtseva, Y.V., Osbun, N. and Shippen, D.E. (2005) The Arabidopsis Pot1 and Pot2 proteins function in telomere length homeostasis and chromosome end protection. *Mol Cell Biol*, 25, 7725-7733.

Shaw, C.J. and Lupski, J.R. (2004) Implications of human genome architecture for rearrangement-based disorders: the genomic basis of disease. *Hum Mol Genet*, 13 Spec No 1, R57-64.

Shay, J.W. and Wright, W.E. (2005) Senescence and immortalization: role of telomeres and telomerase. *Carcinogenesis*, 26, 867-874.

Shay, J.W., Wright, W.E. and Werbin, H. (1991) Defining the molecular mechanisms of human cell immortalization. *Biochim Biophys Acta*, 1072, 1-7.

Shippen-Lentz, D. and Blackburn, E.H. (1990) Functional evidence for an RNA template in telomerase. *Science*, 247, 546-552.

Shrivastav, M., De Haro, L.P. and Nickoloff, J.A. (2008) Regulation of DNA double-strand break repair pathway choice. *Cell Res*, 18, 134-147.

Siroky, J., Zluvova, J., Riha, K., Shippen, D.E. and Vyskot, B. (2003) Rearrangements of ribosomal DNA clusters in late generation telomerase-deficient Arabidopsis. *Chromosoma*, 112, 116-123.

Slijepcevic, P. (2006) The role of DNA damage response proteins at telomeres--an "integrative" model. *DNA Repair,* 5, 1299-1306.

Smogorzewska, A. and de Lange, T. (2004) Regulation of telomerase by telomeric proteins. *Annu Rev Biochem,* 73, 177-208.

Smogorzewska, A., Karlseder, J., Holtgreve-Grez, H., Jauch, A. and de Lange, T. (2002) DNA ligase IV-dependent NHEJ of deprotected mammalian telomeres in G1 and G2. *Curr Biol,* 12, 1635-1644.

Smogorzewska, A., van Steensel, B., Bianchi, A., Oelmann, S., Schaefer, M.R., Schnapp, G. and de Lange, T. (2000) Control of human telomere length by TRF1 and TRF2. *Mol Cell Biol,* 20, 1659-1668.

Son, N.H., Murray, S., Yanovski, J., Hodes, R.J. and Weng, N. (2000) Lineage-specific telomere shortening and unaltered capacity for telomerase expression in human T and B lymphocytes with age. *J Immunol,* 165, 1191-1196.

Stansel, R.M., de Lange, T. and Griffith, J.D. (2001) T-loop assembly in vitro involves binding of TRF2 near the 3' telomeric overhang. *Embo J,* 20, 5532-5540.

Teixeira, M.T., Arneric, M., Sperisen, P. and Lingner, J. (2004) Telomere length homeostasis is achieved via a switch between telomerase- extendible and -nonextendible states. *Cell,* 117, 323-335.

Trask, B., van den Engh, G., Mayall, B. and Gray, J.W. (1989) Chromosome heteromorphism quantified by high-resolution bivariate flow karyotyping. *Am J Hum Genet,* 45, 739-752.

Tsuji, H., Ishii-Ohba, H., Katsube, T., Ukai, H., Aizawa, S., Doi, M., Hioki, K. and Ogiu, T. (2004) Involvement of illegitimate V(D)J recombination or microhomology-mediated nonhomologous end-joining in the formation of intragenic deletions of the Notch1 gene in mouse thymic lymphomas. *Cancer Res,* 64, 8882-8890.

Uegaki, K., Adachi, N., So, S., Iiizumi, S. and Koyama, H. (2006) Heterozygous inactivation of human Ku70/Ku86 heterodimer does not affect cell growth,

double-strand break repair, or genome integrity. *DNA Repair (Amst)*, 5, 303-311.

Underwood, D.H., Carroll, C. and McEachern, M.J. (2004) Genetic dissection of the Kluyveromyces lactis telomere and evidence for telomere capping defects in TER1 mutants with long telomeres. *Eukaryot Cell*, 3, 369-384.

van Steensel, B. and de Lange, T. (1997) Control of telomere length by the human telomeric protein TRF1. *Nature*, 385, 740-743.

van Steensel, B., Smogorzewska, A. and de Lange, T. (1998) TRF2 protects human telomeres from end-to-end fusions. *Cell*, 92, 401-413.

Vogel, H., Lim, D.S., Karsenty, G., Finegold, M. and Hasty, P. (1999) Deletion of Ku86 causes early onset of senescence in mice. *Proc Natl Acad Sci U S A*, 96, 10770-10775.

von Zglinicki, T., Pilger, R. and Sitte, N. (2000) Accumulation of single-strand breaks is the major cause of telomere shortening in human fibroblasts. *Free Radic Biol Med*, 28, 64-74.

Waldman, A.S., Tran, H., Goldsmith, E.C. and Resnick, M.A. (1999) Long inverted repeats are an at-risk motif for recombination in mammalian cells. *Genetics*, 153, 1873-1883.

Walmsley, R.M. and Petes, T.D. (1985) Genetic control of chromosome length in yeast. *Proc Natl Acad Sci U S A*, 82, 506-510.

Wang, E. (1995) Senescent human fibroblasts resist programmed cell death, and failure to suppress bcl2 is involved. *Cancer Res*, 55, 2284-2292.

Watson, J.D. (1972) Origin of concatemeric T7 DNA. *Nat New Biol*, 239, 197-201.

Watson, J.D. and Crick, F.H. (1953) The structure of DNA. *Cold Spring Harb Symp Quant Biol*, 18, 123-131.

Wei, C., Skopp, R., Takata, M., Takeda, S. and Price, C.M. (2002) Effects of double-strand break repair proteins on vertebrate telomere structure. ***Nucleic Acids Res*****, 30, 2862-2870.**

Wicky, C., Villeneuve, A.M., Lauper, N., Codourey, L., Tobler, H. and Muller, F. (1996) Telomeric repeats (TTAGGC)n are sufficient for chromosome capping function in Caenorhabditis elegans. ***Proc Natl Acad Sci U S A*****, 93, 8983-8988.**

Wilkie, A.O., Higgs, D.R., Rack, K.A., Buckle, V.J., Spurr, N.K., Fischel-Ghodsian, N., Ceccherini, I., Brown, W.R. and Harris, P.C. (1991) Stable length polymorphism of up to 260 kb at the tip of the short arm of human chromosome 16. ***Cell*****, 64, 595-606.**

Wilson, R.K. (1999) How the worm was won. The C. elegans genome sequencing project. ***Trends Genet*****, 15, 51-58.**

Wright, W.E. and Shay, J.W. (1992) The two-stage mechanism controlling cellular senescence and immortalization. ***Exp Gerontol*****, 27, 383-389.**

Wright, W.E., Tesmer, V.M., Huffman, K.E., Levene, S.D. and Shay, J.W. (1997) Normal human chromosomes have long G-rich telomeric overhangs at one end. ***Genes Dev*****, 11, 2801-2809.**

Wu, G., Lee, W.-H. and Chen, P.-L. (2000) NBS1 and TRF1 Colocalize at Promyelocytic Leukemia Bodies during Late S/G2 Phases in Immortalized Telomerase-negative Cells. IMPLICATION OF NBS1 IN ALTERNATIVE LENGTHENING OF TELOMERES. ***J. Biol. Chem.*****, 275, 30618-30622.**

Yang, Q., Zheng, Y.L. and Harris, C.C. (2005) POT1 and TRF2 cooperate to maintain telomeric integrity. ***Mol Cell Biol*****, 25, 1070-1080.**

Yasumoto, S., Kunimura, C., Kikuchi, K., Tahara, H., Ohji, H., Yamamoto, H., Ide, T. and Utakoji, T. (1996) Telomerase activity in normal human epithelial cells. ***Oncogene*****, 13, 433-439.**

Yeager, T.R., Neumann, A.A., Englezou, A., Huschtscha, L.I., Noble, J.R. and Reddel, R.R. (1999) Telomerase-negative immortalized human cells contain a novel type of promyelocytic leukemia (PML) body. ***Cancer Res*****, 59, 4175-4179.**

Yu, X. and Gabriel, A. (2003) Ku-dependent and Ku-independent end-joining pathways lead to chromosomal rearrangements during double-strand break repair in Saccharomyces cerevisiae. *Genetics*, 163, 843-856.

Zetka, M.C. and Rose, A.M. (1992) The meiotic behavior of an inversion in Caenorhabditis elegans. *Genetics*, 131, 321-332.

Zhang, Q., Williams, E.S., Askin, K.F., Peng, Y., Bedford, J.S., Liber, H.L. and Bailey, S.M. (2005) Suppression of DNA-PK by RNAi has different quantitative effects on telomere dysfunction and mutagenesis in human lymphoblasts treated with gamma rays or HZE particles. *Radiat Res*, 164, 497-504.

Zhang, Y., Zhou, J., Cao, X., Zhang, Q., Lim, C.U., Bailey, S.M., Ullrich, R.L. and Liber, H.L. (2006) Partial deficiency of DNA-PKcs increases ionizing radiation-induced mutagenesis and telomere instability in human cells. *Cancer Lett.*

Zhao, Y., Hoshiyama, H., Shay, J.W. and Wright, W.E. (2008) Quantitative telomeric overhang determination using a double-strand specific nuclease. *Nucleic Acids Res*, 36, e14.

Zhong, Q., Chen, C.F., Chen, P.L. and Lee, W.H. (2002) BRCA1 facilitates microhomology-mediated end joining of DNA double strand breaks. *J Biol Chem*, 277, 28641-28647.

Zhu, L., Hathcock, K.S., Hande, P., Lansdorp, P.M., Seldin, M.F. and Hodes, R.J. (1998) Telomere length regulation in mice is linked to a novel chromosome locus. *Proc Natl Acad Sci U S A*, 95, 8648-8653.